MEDIRAD

Project title: Implications of Medical Low Dose Radiation Exposure

Grant Agreement Number: 755523

Call identifier: NFRP-2016-2017

Topic: NFRP-9

Deliverable 2.19

Report on effectiveness of protective devices for staff in interventional procedures

Lead partner: Belgian Nuclear Research Centre (SCK CEN)

Author(s): Jérémie Dabin, Joanna Domienik-Andrzejewska, Christelle Huet, Mateusz Mirowski, Filip Vanhavere

Work Package: 2

Estimated delivery: 31 December 2020

Actual delivery: 8 January 2021

Type: Report

Dissemination level: Public

This project has received funding from the Euratom research and training programme 2014-2018 under grant agreement No 755523.

Table of contents

List of figures

List of tables

Abbreviations

CRYA: Cryoablation

CTO: Chronic total occlusion

FT: Fluoroscopy time

IC: interventional cardiology procedures

ICRP: International Commission on Radiological Protection

$K_{a,r}$: cumulative air-kerma at patient entrance reference point

P_{KA}: Kerma-area product

LAO: Left anterior oblique

LDL: Lowest detection limit

LLAT: Left lateral

MC: Monte Carlo

MCNP: Monte Carlo N-Particle

ORNL: Oak Ridge National Laboratory

PA: Posterior-anterior

PCI: Percutaneous coronary interventions

RA: Rando Alderson

RAF: Realistic anthropomorphic flexible

RAO: Right anterior oblique

RFA: Radiofrequency ablation

RLAT: Right lateral

RP: Radioprotective

TLD: thermoluminescent dosimeters

WB: whole body

ZG: Zero Gravity

1. Introduction

Since the early 2010s, several studies have reported an elevated incidence of eye lens opacities typically associated with ionising radiations among hospital interventional staff (Ciraj-Bjelac *et al.*, 2010; Vano *et al.*, 2013). Recent publications have reported other potential hazards. Roguin (Roguin *et al.*, 2012; Roguin *et al.*, 2013) reported a possible association with brain tumours. Andreassi found subclinical carotid atherosclerosis (Andreassi *et al.*, 2015) and, more generally, health problems (Andreassi *et al.*, 2016).

Many devices exist to protect the staff from radiation exposure. The lead apron, often combined with a lead collar, remains the standard individual equipment. Table lead curtains and ceiling-suspended screen have become conventional room equipment, at least in interventional cardiology (IC, Domienik-Andrzejewska *et al.*, 2018). Other radioprotective (RP) devices exist such as drapes positioned on the patient, caps or various types of cabins. However, estimating the actual efficiency of those devices remains challenging because it can be strongly affected by their design and the exposure conditions.

Among other activities, the MEDIRAD project (Implications of medical low dose radiation exposure) aims to bridge gaps in the knowledge of staff radiation protection. The efficiency of novel equipment to protect the staff, and particularly the eye lens and the brain, was investigated. Caps, lead-free aprons, drapes covering the patient, masks and a novel ceiling-suspended system were thoroughly investigated by means of Monte Carlo (MC) simulations validated through clinical measurements on the staff and phantoms.

2. Material and Methods

2.1 Selection of the radioprotective devices

The RP devices to be investigated were selected based on an extensive literature review of the devices available to the staff during fluoroscopically-guided procedures. It was aimed at establishing an exhaustive list of devices, covering frequently encountered ones such as lead glasses or ceiling-suspended screen, as well as more novel ones such as lead masks or ceiling suspended apron system. Only equipment mounted devices and personal protective devices were considered, hence excluding architectural shielding (i.e. build into the operative room walls). In total, 67 articles, were gathered, in the recent scientific literature (from 2000 on); among which 59 were of particular interest (list see annex). Those were reviewed according to 10 criteria (type of RP devices, shielded region, efficiency, type of procedures, ease of use, trustworthiness of the publications, etc.), with a specific attention to devices which protect the eye lens and the brain of the staff. About ten different types of devices were identified (Table 1), with some articles focusing on more than one type of device. The most studied ones were RP drapes (39% of the articles), ceiling suspended screen (21%) and lead glasses (16%); five articles (8%) presented novel suspended systems intended to replace the personal apron of the first operator.

Table 1: Frequency of the protection devices studied in scientific papers

	Drapes (lead/non lead)	ceiling suspended screen	Lead glasses	Cap	Table skirt	Table vertical extension	Aprons (lead/non lead)	Hood	Thyroid collar	Suspended systems	Mask
#	24 (7; 17)	13	10	6	6	5	4 (4; 3)	3	2	5	1
%	39% (11%; 28%)	21%	16%	10%	10%	8%	6% (6%; 5%)	5%	3%	8%	2%

Based on this literature search and the authors' experience, a need for additional investigations was identified for the RP caps, masks, drapes, lead-free aprons and the Zero Gravity, a suspended lead apron system. An explanation on why these were specifically chosen can be found below. Within MEDIRAD, the lead glasses and the ceiling-suspended screen, which are nowadays conventional shielding devices in IC, were not selected. Both devices, and sometimes their combined use, have been extensively studied over the years. It is commonly agreed that the ceiling-suspended screen, when used properly, has the potential to significantly reduce the exposure of all shielded organs, including the hands, the eye lens and the brain. Well-designed lead glasses are an efficient device to protect the eye lens. A few studies also investigated the effect of lead glasses on the brain exposure. As it could be expected, their efficiency was very limited.

For these five devices, the RP efficiency was extensively investigated by means of MC simulations validated through measurements on the staff and phantoms.

2.2 Radioprotective devices

Caps

Various RP cap models are commercially available (Figure 1). Clinical studies (Karadag *et al.*, 2013; Alazzoni *et al.*, 2015; Sans Merce *et al.*, 2016) have recently investigated their efficiency (only covering the upper part of the head (Figure 1, left)). Dosimeters were usually placed over the caps and underneath, in contact with the staff skin, to extrapolate the dose savings to the brain. Unfortunately,

a recent study (Honorio da Silva *et al.*, 2020) has shown that this methodology alone was not sufficient to assess the dose savings to the brain, and that measurements had to be coupled with simulations.

Figure 1: Pictures of two commercially available RP cap models: X-Ray Protective Cap (left; MAVIG; source: https://mavig.com) and RADPAD No Brainer X-ray Protective Surgical Cap (right; Worldwide Innovations & Technologies; source: http://www.varaylaborix.com).

Masks

Although RP face masks have been available for decades (Figure 2), only one publication studying the efficiency of lead masks was found (Marshall *et al.*, 1992). Unfortunately, the study only considered the attenuation characteristics in laboratory conditions, which can significantly differ from clinical practice.

Figure 2: Pictures of two commercially available RP face mask models: VIS400 face mask (left; source: www.varaylaborix.com) and Full face style mask (right; Philips Safety products, source: www.phillips-safety.com).

Drapes

Lead or lead-free drapes placed on the patient outside the x-ray primary beam (Figure 3) are relatively new compared to other standard RP devices such as the lead apron or the thyroid collar. Nevertheless, numerous studies (24, most of which being clinical) on the efficiency of lead or lead-free RP drapes covering the patients were identified. The dose reduction to the eye lens was assessed in some cases but the potential dose savings to the brain were not. Besides, no publication included results of MC simulation studies, which can be of invaluable help to investigate the drape limitations and optimise their use.

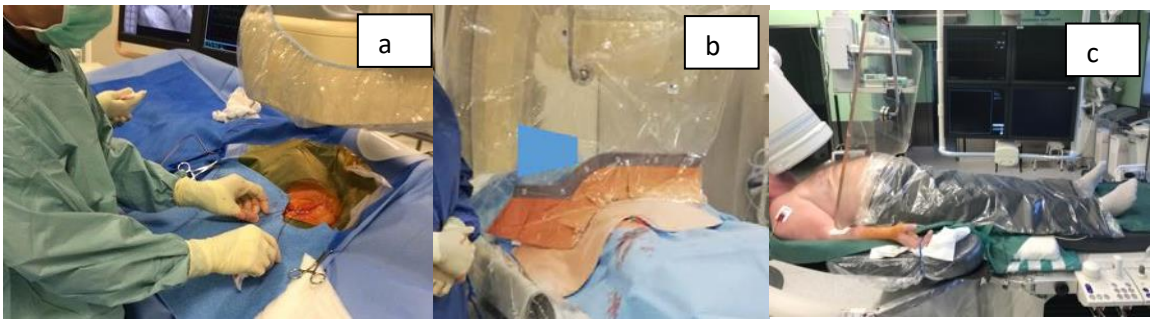

Figure 3: Pictures of two commercially available lead-free drape models: (a) RADPAD subclavian shield (left, Worldwide Innovations & Technologies; source: www.radpad.com), (b) radial X-ray protection drape (right; MAVIG; source: (McCutcheon *et al.*, 2020)) and (c) lead drape of 0.5mmPb and size of 80x100cm (LITE TECH, INC., USA).

Aprons

Although four studies investigating the efficiency of lead and lead-free aprons (Figure 4) could be found, they were all performed in the laboratory or on phantoms. Therefore, it is needed to evaluate the efficiency of lead-free aprons in real clinical conditions, which can strongly differ from the ideal laboratory conditions.

Figure 4: Pictures of two commercially available apron models: Vest and Skirt Wrap and thyroid collar (left, Scanflex; source: www.scanflex.se) and Balance vest and skirt (right; MAVIG; source: www.mavig.com).

Zero-Gravity suspended system

The Zero-gravity (ZG, Biotronik, Germany) is certainly the most recent RP device among the reviewed ones. It is a fully suspended system (Figure 5) composed of an apron with increased lead thickness (0.5 to 1 mm Pb depending on the location) equipped with lead flaps over the upper arms and a lead face shield (0.5 mm Pb).Although it looks like a promising solution to the back-pain issue caused by lead aprons, the ZG system is only in use in a limited number of hospitals. Only five studies of its efficiency were found, including three studies on staff. No MC simulation studies were found. The information on dose reduction to the eye lens was limited, and no information on brain dose reduction was available.

Figure 5: Pictures of the Zero Gravity suspended radiation protection system (Worldwide Innovations & Technologies): Floor Unit suspended system (left; source: www.biotronik.com) and clinical use (right; source:(Savage *et al.*, 2013)).

2.3 Monte Carlo simulations

Monte Carlo simulations were performed for all simulated devices to calculate their potential for reducing exposure of various organs in set-ups commonly used during interventional procedures. In addition, dosimeters were modelled to investigate the correlation between the real shielding efficiency (calculated at the level of the organs) and the efficiency as estimated from measurements on staff (calculated at the level of the dosimeters).

Monte Carlo code and calculation settings

A geometry representative of an IC setup was simulated using the MC code MCNPX 2.7 and MCNP6.2 (Los Alamos National Laboratory, USA). The DXTRAN variance reduction method was used where needed. This method enables the number of particles to be increased in the region of interest. Tests have been conducted in order to ensure that the results with and without the DXTRAN sphere were in agreement and so that using the DXTRAN method does not lead to pronounced bias.

The energy deposition in the organs, tissues and dosimeters of interest was calculated using F6:p tally, which calculates the average energy deposited by photons over a cell. Energy from electrons created by photon interactions is assumed to be deposited locally. Validity of this assumptions was verified through simulations using the *F8 tally, which calculates energy deposition without relying on the local energy deposition assumption. For the drape, the apron and the ZG system, the effective dose was calculated applying ICRP 103 (2007) formalism on the organ and tissue doses.

Interventional cardiology set-up

Interventional cardiology set-ups combining eight examination parameter settings, which were representative of IC, were simulated. The settings are listed in Table 2. Five x-ray beam projections were considered, namely postero-anterior (PA), left anterior oblique at 45° and 90° (LAO 45 and LLAT, respectively) and right anterior oblique at 45° and 90° (RAO45 and RLAT, respectively). Two positions of the operator with respect to the centre of the x-ray field (40 cm and 70 cm) were studied, except for the ZG device which could not be positioned at 40 cm due to its bulkiness. Two orientations of the operator's head were modelled: forward and 30° away from the x-ray source. The source-to-image-detector distance was fixed (90 cm); the source-to-patient-entrance distance and the patient-to-image-detector distance was set to 60 cm and 10 cm in PA, respectively, and could differ after beam rotation depending on the dimensions of the patient model's.

The x-ray tube was represented as a point source collimated towards the patient chest and projecting a square field size (20x20 cm² or 30x30 cm²) on the image intensifier. An x-ray spectrum corresponding to a tube voltage of 80 kVp with a total filtration of 3 mm Al was used. It was assumed that the beam quality would have little influence on the device efficiency as observed by Koukorava et al. (2011 and 2014). The image intensifier was represented as a simple parallelepiped lead box with an entrance window made of 1.5 mmAl. No patient bed nor RP room equipment was modelled since these were assumed to have a negligible effect on the efficiency of the studied device.

Table 2: Interventional cardiology set-ups implemented in the MC simulations

Examination settings	Values
Use of RP device	With - without
Beam projections	PA, LAO 45, LLAT, RAO45, RLAT
Operator´s distance from the x-ray field	40 and 70 cm
Operator´s head orientation	forward (0°) and 30° away from the x-ray source
Field size at the detector (cm)	30 x 30: PA, LAO 45 and RAO 45 20 x 20: LLAT and RLAT
X-ray energy spectrum	80 kVp, 3mm Al
Source-to-patient distance (cm)	60
Source-to-image-detector distance (cm)	90
Patient-to-image-detector distance (cm)	10

Patient and staff modelling

One simplified phantom model was used for representing the patient while three different phantom models, all representing a 176 cm reference person, were used for the cardiologist depending on the organs under investigations and the need for more realistic representation. The RP devices under investigation and the phantom models are listed in Table 3.

A simplified version of the Oak Ridge National Laboratory (ORNL) - ORAMED phantom (Koukorava et al., 2011) was used to represent the patient. This phantom only contains a simplified skeleton and lungs; all remaining organs are modelled as homogenous tissue.

For the study of the masks, the caps and drapes, the cardiologist was modelled as the ORNL - ORAMED phantom completed with a voxelised head (Zubal *et al.*, 1994), as in (Silva *et al.*, 2017), which was specially modified to include a detailed eye lens structure following Behrens's model (Behrens *et al.*, 2009). This newly created phantom allowed the calculation of the deposited dose to detailed substructures of the brain and the eye (Figure 6).

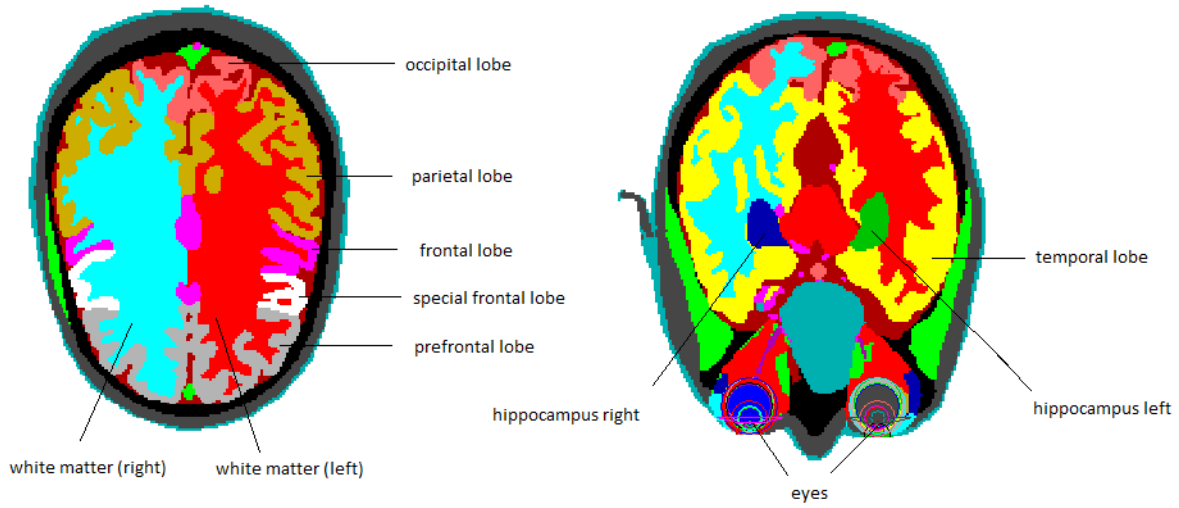

Figure 6: Voxelised head phantom including detailed brain and eye lens structures.

The ICRP male phantom (ICRP, 2009) equipped with an apron, from Saldarriaga Vargas (Saldarriaga Vargas *et al.*, 2018), was used for the study of the lead-free aprons. A ZG system was specially modified to equip the realistic anthropomorphic flexible (RAF) phantom (Lombardo et al., 2018).

Table 3: Target organs and staff models implemented in the MC simulations

RP device	Target organs	Phantom
Mask	Brain tissue and eye lens	ORNL-ORAMED phantom with a voxelised head and a detailed eye lens model
Lead-free and leaded caps	Brain tissue	Same as for the mask
RP drapes	All organs; hands	Same as for the mask but with hands on the patient
Lead-free and light-lead aprons	All organs under the apron	ICRP male phantom equipped with an apron
Zero-gravity system	All organs	RAF phantom equipped with a ZG system

Radioprotective device modelling

Caps

The cap was modelled based on a commercial surgical model (RADPAD No Brainer X-ray Protective Surgical Cap; Worldwide Innovations & Technologies) which is 12 cm high and covers the head obliquely from above the nape to the top of eyebrows (Figure 7). The top of the head is unshielded. Two compositions were considered: pure lead and lead-free.

In the literature, clinical studies have investigated the dose reduction potential of caps relying on simultaneous measurements above and under the cap (Alazzoni *et al.*, 2015; Sans Merce *et al.*, 2016). Three pairs of dosimeters made of soft tissue material were therefore modelled above and under the cap (Figure 7) in order to verify their relevance for efficiency studies. They were placed near the left temple, at the forehead between the eyes and at the end of the left eyebrow. An eye lens ($H_p(3)$) dosimeter was also modelled on the left temple.

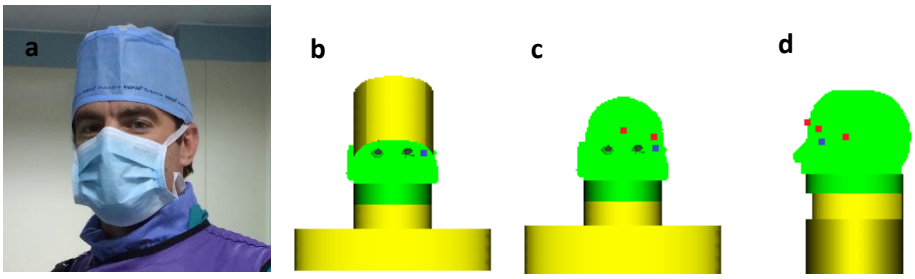

Figure 7: a: Cap modelled in the MC simulations (RADPAD No Brainer X-ray Protective Surgical Cap; Worldwide Innovations & Technologies; source: http://www.varaylaborix.com). b: frontal view of the cardiologist model with the cap. c and d: frontal and lateral view of the cardiologist model without the cap; dosimeters are represented in red (soft tissue) and blue (eye lens).

Masks

Among the several designs of masks commercially available, two of them (VIS400 face mask (manufacturer unknown) and Full face style mask (Philips Safety products, USA)) were selected and modelled (Figure 8); those masks are named M1 and M2 in the rest of the report. Since both are composed of unknown proportions of acrylic and lead, they were modelled using the lead equivalence announced by the manufacturer (0.1 mm Pb). In addition, to further investigate the effect of design, a third mask (named M1L) was modelled as M1 with a 7.8 cm longer screen, so that it had the same length as M2.

As for the caps, pairs of dosimeters placed under and below the mask were modelled to evaluate the relevance of such measurements in clinical practice. Four pairs of detectors were modelled as cylinders (0.16 cm^3) made of soft tissue material at the four extremities of the masks M1 and M2. An eye lens ($H_p(3)$)dosimeter was modelled on the left temple.

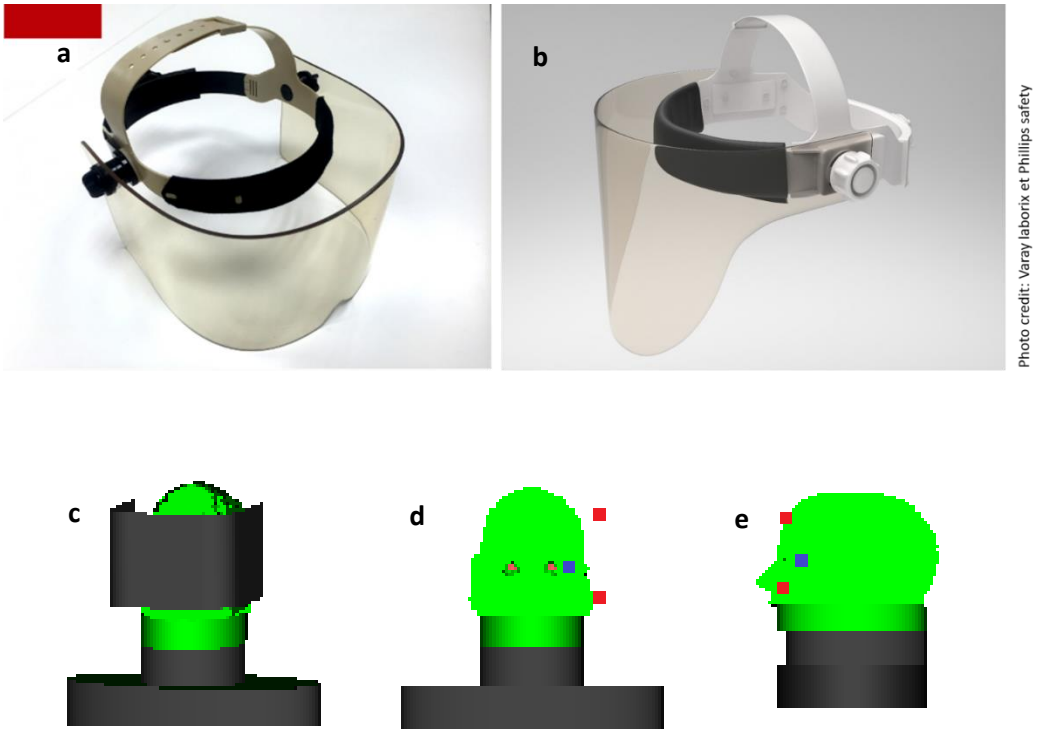

Figure 8:a and b: Pictures of the commercial masks modelled in the MC simulations (M1 on the left, M2 on the right). e: frontal view of the cardiologist model with the M1 mask. d and e: frontal and lateral view of the cardiologist model without the mask; dosimeters are represented in red (soft tissue dosimeters positioned on the mask) and blue (eye lens).

Drapes

Two different models of a commercially available lead-free drapes (RADPAD Red Label (0.375 mm Pb eq) femoral entry and multipurpose shields, Worldwide Innovations & Technologies, USA) were modelled. The drape extended slightly left from the centre of the patient abdomen until the right side of the table, as illustrated in Figure 9. Both models only differed by the presence of a hole at the right bottom of the model used in femoral access when the cardiologist is positioned at 70 cm from the centre of the primary x-ray beam (Figure 10, two right images).

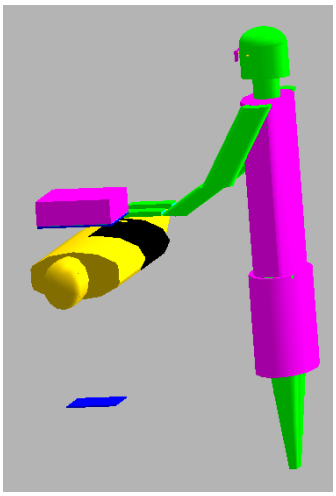

Figure 9: Reference position of the patient drape (in black) during MC simulations

The material composition was obtained in confidence from the manufacturer. Although the manufacturer advised different drape positions depending on the access route (represented in the MC simulations by staff position with respect to the x-ray beam centre), this could not be implemented. Positioning the drape closer to the patient chest as advised for a radial or brachial access route would have resulted in the drape interacting with the primary beam. Only one drape position was therefore considered for the main simulation set-ups as described in Table 2. Extremity ($H_p(0.07)$) dosimeters were modelled on the cardiologist's hands and forearms. An eye lens ($H_p(3)$) dosimeter was modelled on the left temple and a whole-body (WB, $H_p(10)$) dosimeter on the left side of the chest above the apron.

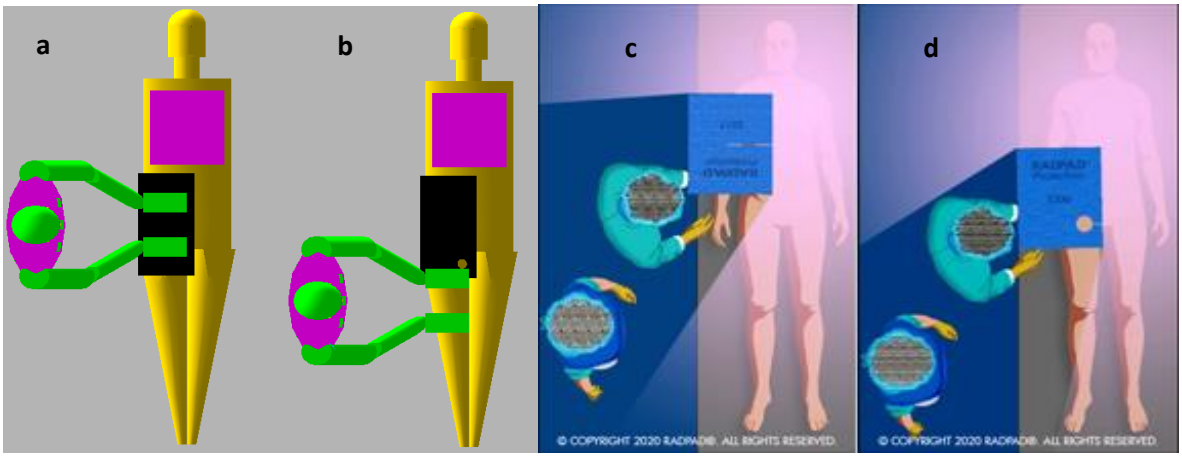

Figure 10:a and b: Top view from the ORNL-ORAMED phantoms used for investigation of drape efficiency. The cardiologist is positioned at 40 cm (left) and 70 cm (right) from the x-ray beam centre. Radioprotective drape is coloured in black. c and d: Top view from the Radpad drape position for brachial and radial (left) and femoral accesses (right) as advised by the manufacturer (http://radpad.com/products/).

The effect of drape dimensions and positions was assessed for limited set-ups for a PA projection and compared with the femoral entry shield. Four additional pad positions implementing5 cm shifts perpendicular to the patient (i.e. towards or away from the cardiologist) and parallel to the cardiologist (towards or away from the patient's head) as per Figure 11. Three additional designs, which represent different patient coverage parallel or perpendicular to the patient as per Figure 12, were modelled.

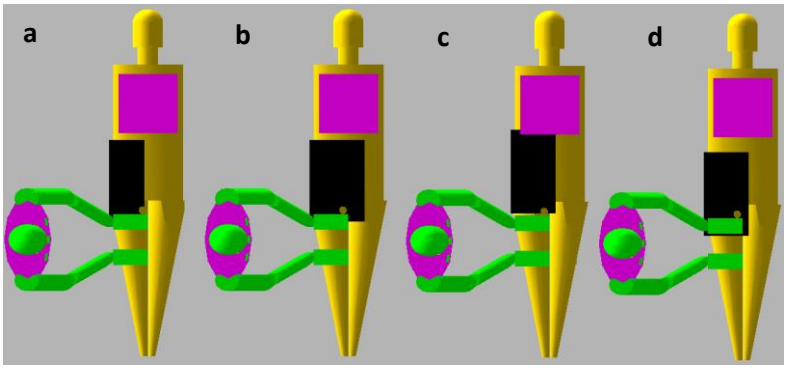

Figure 11: Sensitivity study of four additional drape positions: 5 cm shift towards the cardiologist (a), away from the cardiologist (b), towards the patient's head (c) and away from the patient's head (d).

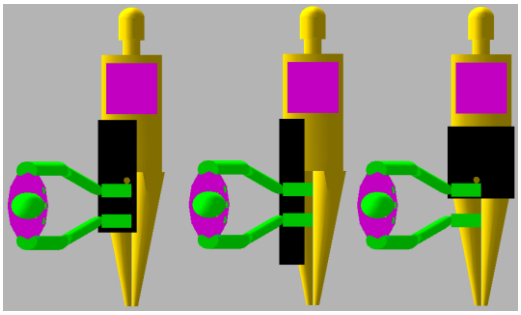

Figure 12: Sensitivity study of three additional drape dimensions

Aprons

Three full-body apron models with different compositions were studied. Pure lead and two lead-free compositions, based on manufacturer data (LFA1) and on data from experimental characterisation (LFA2) (Aral *et al.*, 2020), were modelled (Table 4).

Table 4: Characteristics of the modelled lead and lead-free aprons

Apron	Composition	Density	Thickness(mm)
Lead apron (LA)	Pb	11.35	0.5
Lead-free apron 1 (LFA1)	Sb + Bi	4.8	0.5
Lead-free apron 2 (LFA2)	Sb + BI	3.3	1.2

All aprons and thyroid collar had the same design; only the effect of the material composition and/or the actual thickness were considered (Figure 13). For each apron, a thyroid collar with the same thickness and composition was also modelled.

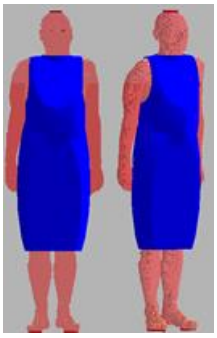

Figure 13: ICRP phantom equipped with a radioprotective apron used for investigation of lead and lead-free apron efficiency

Zero-Gravity suspended system

The ZG was modelled based on the information provided by the manufacturer: an apron with lead thickness varying between 0.5 to 1 mm for the apron and the arm flaps, depending on the location, and 0.5 mm for the face shield. The model was then included in a software enabling fast generation of MCNP input files (Figure 14)(Lombardo and Zankl, 2018). As already mentioned, due to its bulkiness it was not possible to position the operator at 40 cm from the source. A WB ($H_p(10)$) dosimeter was added on the left side of the cardiologist chest, above the apron when worn, and below the ZG otherwise.

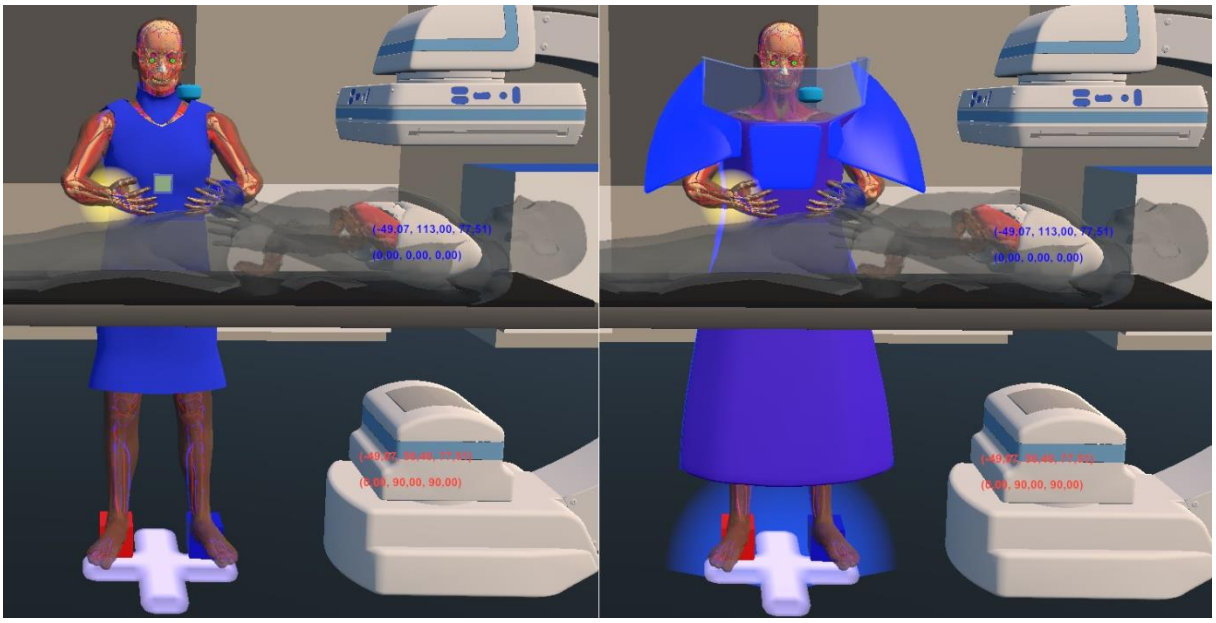

Figure 14: Flexible numerical phantom equipped with an apron (left) and with the ZG system (right) as modelled in IPP

2.4 Staff monitoring

Monte Carlo simulations are the reference method for accurately calculating the efficiency of RP devices but only limited, static configurations can be investigated. In clinical practice, however, the RP devices are used in a large variety of configurations.

Clinical measurements were performed for each RP device in at least two hospitals in Belgium and Poland. For the mask, however, no clinical measurements were performed because no cardiologist who were willing to participate in the study was found during the project duration. The outbreak of the COVID-19 pandemic prevented from enrolling potential participants outside the partner countries.

Each measurement campaign consisted in monitoring the staff with (RP group) and without the studied RP device (Control group) for identical periods or number of procedures. All other RP measures or devices conventionally used in clinical practice were used as in normal practices. Only diagnostic and therapeutic percutaneous coronary interventions (PCI) were considered; except for one device also used in one hospital during cryoablations (CRYA) and radiofrequency ablations (RFA). Procedures matching the inclusion criteria were attributed to the RP or Control group following a random[1] or sequential inclusion strategy[2]. . Finally, cardiologists were not blind to the use of the RP device.

Depending on the organs of interest, dedicated WB, eye lens and extremity dosimeters were used, possibly with loose detectors at complementary positions of interest. In general, WB dosimeters were worn above the apron, if an apron was used, on the left side of the chest; ring dosimeters were worn on both ring fingers; and eye lens dosimeters were worn on the left temple. WB, eye lens, and extremity dosimeters were calibrated according to International Organization for Standardization (ISO; Geneva, Switzerland) norms N60, N80or N100 reference beam (ISO 2004), depending on beam availability and local specificities at the measurement site, against personal dose equivalent $H_p(10)$, $H_p(3)$ and $H_p(0.07)$, respectively. In particular, all dosimeters used at a specific site (both for Control and RP groups) were calibrated using the same reference beam. The lowest detection limit (LDL) was either determined from previous characterisation studies or as three times the standard deviation from the readings of background dosimeters.

Measurement results were also normalised to the dose-area product (P_{KA}) when available. Details of the clinical measurements are described individually for each RP device below and summarised in Table 5.

Details of the measurement campaigns are described separately for each RP device.

Table 5: Summary of the measurements for each RP device. N_{RP} and N_C are the number of procedures monitored with (RP group) and without using the considered device (Control group), respectively. For the light lead and lead-free apron, N_{RP} and N_C are the monitoring months cumulated over all participants cardiologists. N_{RP} is the cumulative number of months when a lead-free or a light lead apron was worn; N_C is the cumulative number of months when a lead apron was worn. Dr is the number of cardiologists participating in the measurement campaign. For the aprons, the number of cardiologists in each study group is reported. Diagnostic and therapeutic PCI procedures were monitored in all hospitals but hospital J where RFA and CRYA procedures were monitored.

RP device	Hosp	N_{RP}	N_C	Dr	Dosimeters
Lead(-free) cap	A (phase 1)	30 proc	-	3	9 TLDs on head: 6 TLDs under lead-free cap, 3 outside

[1]Procedures were randomly allocated to the RP or Control group until both groups achieved a determined size.
[2]Procedures were allocated to the Control group until a determined group size was achieved, then procedures were allocated to the RP group until achieving an identical size.

	A (phase 2)	291 proc	-	4	6 TLDs on head: 3 TLDs under lead-free cap, 3 outside
	B	>3 months	>3 months	1	20 TLDs on head, WB
	C	>1 months	>1 months	1	
Lead and lead-free drapes	D	318 proc	314 proc	7	WB, left eye lens and 2 rings
	E	30 proc	32 proc	4	
Light lead and lead-free apron	F	88months	620 months	11 &15	WBabove and under apron
	G	193months	-	5	
	H	63months	379 months	7 & 9	
Zero-Gravity suspended system	I	25	25	3	WB, left eye lens, left upper-arm and 2 rings
	J*	39	-	4	WB, left eye lens, and 2 rings
	K	69	82	2	WB, left eye lens, and 2 rings

Caps

In hospital A, the participating cardiologists wore dosimeters both on and under the lead-free cap, there was therefore no control group. The measurements were performed in 2 phases. In the first phase, three cardiologists participated in the study and the measurements were performed per single procedure; and in total 30 procedures were performed. Cardiologists wore a lead-free cap (RadPad, 0.25 mm Pb). Six high-sensitivity thermoluminescent dosimeters (TLDs) type MCP-N (Radcard, Poland) were attached at various locations on the cap (Figure 15): three of them on the forehead at the level of eye brows (two TLDs near the temples and one in the middle of the forehead), one on the top of the head, one on the back of the head near the neck and the last one at equal distance from the dosimeter at the back and the dosimeter on the top of the head. Three extra TLDs were attached at the corresponding locations on the forehead inside the cap.

Information on the RP tools used, cumulative dose-metrics (P_{KA}, cumulative air-kerma at patient entrance reference point ($K_{a,r}$) and fluoroscopy time (FT)) as well as patient characteristics were collected at the end of every procedure.

The LDL was equal to 10 µSv. All doses below this limit were replaced with the LDL value, except for measurements for which both doses on and under the lead cap were below LDL; in the latter case the doses were excluded from the analysis. More than 50% of doses measured on the right temple (on the cap or/and under it) were below the LDL. The estimated RP device efficiency could therefore be biased. In order to increase the accuracy, dose measurements during the second phase were cumulated over a median of 20 procedures before the dosimeters were read. In total, 291 CA and/or PCI procedures were monitored. In addition, three dosimeters were attached both on and under the cap in the most exposed locations: on the left temple, in the middle of the forehead and one in between (near to the left eyebrow).

Figure 15: Position of the TLDs placed on the lead-free cap used in hospital A during the second phase.

In hospital B and C, measurements were performed in two phases (control and study phases). During the control phase a simple surgical cap, covered with MCP-N TLDs, was used (thus offering no RP effect). During the study phase, a RP cap was worn above the surgical cap covered with TLDs. In hospital B, one cardiologist wore a lead cap (0.5 mm Pb eq, MDT, The Netherlands) while, in hospital C, one cardiologist wore a lead-free cap (0.25 mm Pb eq, RADPAD No Brainer X-ray Protective Surgical Cap; Worldwide Innovations & Technologies). During both phases, ten TLDs were positioned on each side of the surgical cap (Figure 16), and doses were cumulated during at least three months in hospital B and at least one month in hospital C. Since the cumulative DAP could not be collected, cumulative doses were normalised to the WB dose from a dedicated dosimeter (Inlight, Landauer, United States) worn on the left side of the chest to account for possible difference in workload. Only diagnostic and therapeutic PCI procedures were monitored. The uncertainty (k=1) associated with the measurements was conservatively estimated to be 40% for doses smaller than 40 µSv and 10% for higher ones. The LDL for the WB was 0.050 mSv; for the loose dosimeters the LDL was 0.040 mSv in hospital B and 0.010 mSv in hospital C.

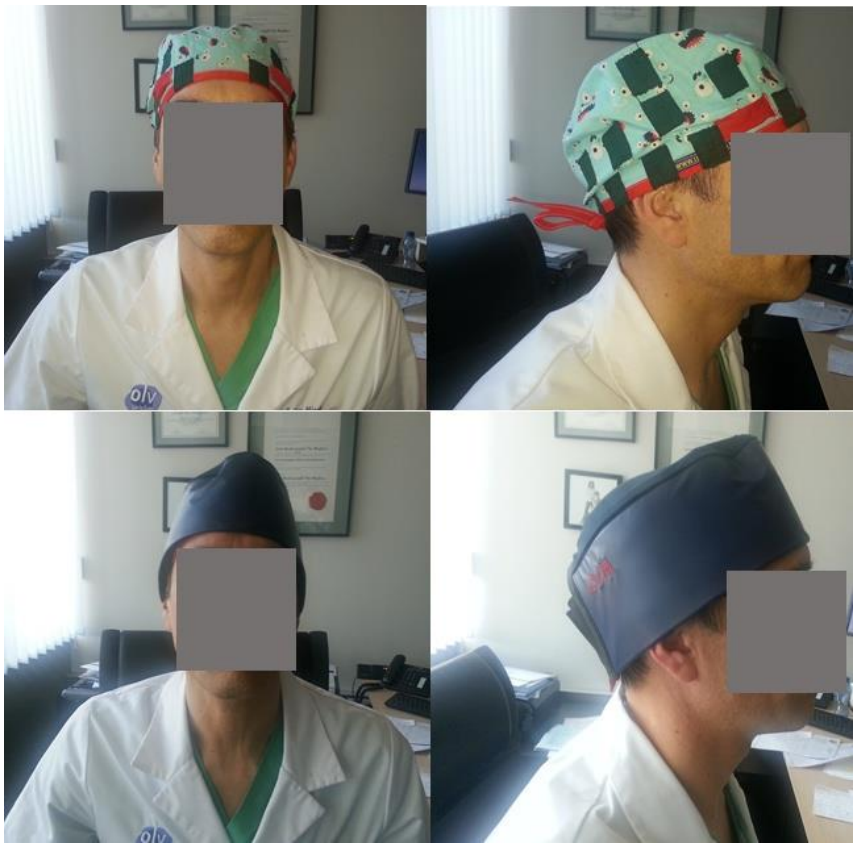

Figure 16: Surgical cap and dosimeter positions as used in hospital B and C (top); lead cap worn in hospital B (bottom).

Drapes

In hospital D, the efficiency of the re-usable MAVIG X-ray protective drapes (MAVIG, Germany) was investigated. Two drape models designed for either femoral or radial access routes, both 0.5 mm Pb eq, were investigated. Seven cardiologists participated in the study. All diagnostic and therapeutic PCI procedures, except PCI for chronic total occlusions, were included and randomly allocated to the study or the control group. Ultimately, 318 patients were included in the study group and 314 in the control group.

Separate sets of dosimeters were available for the study and the control groups. Each set was used for monitoring the cardiologist's exposure cumulated over a median of ten procedures and was shared among the participating cardiologists. Each dosimeter sets were composed of four dosimeters: 2 MCP-N TLDs inserted into ring dosimeters worn on the ring fingers, one into a dedicated eye lens dosimeter (Radcard, Poland) fixed to the left side of the head and one WB dosimeter at the level of the chest on the left side of the apron (Inlight). The uncertainty (k=1) associated with the measurements was conservatively estimated to be 40% for doses smaller than 40 µSv and 10% for higher ones. The LDL for the WB, eye lens and finger dosimeter varied between 0.010 mSv and 0.050 mSv depending on the dosimeter set.

In hospital E, a re-usable lead drape (LITE TECH, INC., USA) with 0.5 mm Pb thickness of standard dimensions 80 cm x 100 cm was used. Three cardiologists participated in the study. All diagnostic and therapeutic PCI procedures were included. Procedures were randomly allocated to the study or the control group. Thirty procedures were included in the study group and 32 in the control group. Dose measurements were performed separately for each procedure using four dosimeters: Two MCP TLDs

inserted into ring dosimeters worn on the ring fingers, one into a dedicated eye lens dosimeter (Radcard) fixed to the left side of the head and one WB dosimeter at the level of the chest on the left side of the apron (Rados TLD). The uncertainty (k=1) associated with the measurements was conservatively estimated to be 40% for doses smaller than 40 µSv and 10% for higher ones. Information on the RP tools used, cumulative dose-metrics (P_{KA}, $K_{a,r}$ and FT) as well as patient characteristics were collected.

Aprons

Eight hospitals were contacted to identify interventional cardiologists who used conventional lead aprons and light lead or lead-free aprons during their career, and for whom routine double dosimetry measurements (i.e. WB dose measurements under and above the apron) could be extracted. TNO badge (The Netherlands) with MTS 100 TLDs (Harshaw, United States of America) were used during the complete period. All dose values smaller or equal to 50 µSv were set to 50 µSv (532 doses), which is a conservative estimate of the LDL.

Ultimately, only data from three hospitals, accounting for 30 cardiologists were useable, 23 of these wore a light lead or lead-free apron and 24 used a lead apron at a moment or another during the monitoring period. The data cover the period 01/12/1999 to 01/10/2018 with a periodicity of one month. A total of 344 months of routine dosimetry follow-up with a lead-free or light lead apron and 999 months of follow-up with a lead apron were collected. For each month, a pair of WB doses above and under the apron was available.

The attenuation of the apron was calculated for each pair of WB doses as per Equation 2.

Zero-Gravity suspended system

In hospital I, three cardiologists participated in the evaluation of the ZG system. Only diagnostic and therapeutic PCI procedures were included. Measurements were performed in two sequential phases (control and study phases). During the control phase, 25 patients were included; 25 were then included during the study phase. Doses were monitored separately for each procedure using: two real-time WB Radiation Insight Raysafe i2 (Unfors RaySafe, Sweden) on the left upper arm, 5 cm above the elbow, and on the left temple close to the eye; two Instadose WB dosimeters worn on the left side of the chest above the apron and on the left side of the thyroid collar; and finger (ring) dosimeters (Radcard) were worn on both ring fingers. The LDL for theRaysafei2, Instadose and finger dosimeter was 0.001mSv, 0.040 mSv and 0.040mSv.

In hospital J, the ZG system is permanently installed in an electrophysiology room. It is the only centre in Poland which owns this system. In hospital K, the system was installed in a haemodynamic room for a trial period of two months. In the electrophysiology room the new system was used simultaneously with the ceiling suspended lead glass and the table curtain. In the haemodynamic room of hospital K, originally equipped with the same radiation covers, the ceiling suspended lead glass was disassembled and its suspension system was used to mount the ZG system for the duration of the measurements. In hospital J, only RFA and CRYA were performed by four cardiologists experienced in working with the ZG system while, in hospital K, diagnostic and therapeutic PCI procedures were performed by two, pre-trained but not experienced, cardiologists. During the study phase, for all measurements except one, the doses were cumulated during few procedures (min. two and max. six) before reading. More than 100 procedures (39 RFA or CRYA and 69 diagnostic and therapeutic PCI procedures) were performed. Three WB dosimeters (Rados) were attached to the left side of the collar, the chest and the waist of every cardiologist (Figure 17). The dedicated eye lens dosimeter was placed on a band near the left eye lens. An extra four loose TL dosimeters were attached to each finger and ankle to evaluate the skin doses in the regions expected not to be protected by the ZG system. The LDL for the WB dosimeter was 0.022 mSv, 0.010 mSv for eye lens and 0.005 mSv for finger and ankle dosimeter. All doses below

LDL were replaced with the appropriate LDL value. More than 90% of measurements performed in the electrophysiology room (all doses measured on the collar, chest, waist and near left eye lens and the majority in the remaining regions) were below LDL as compared with 30% (only on the collar, waist and chest) in the haemodynamic room.

Because of the outbreak of the COVID-19 pandemic during the control phase, no measurements could be performed in the electrophysiology room. Measurements were only done for haemodynamic procedures with the same cardiologists as in the study phase. Eighty procedures were performed with eye lens and left and right finger dosimeters but only 30 of them with an additional WB dosimeter placed on the left side of the chest. The corresponding doses normalized to P_{KA} were compared.

Figure 17: Position of the dosimeters in hospital J for assessment of the ZG suspended system efficiency

2.5 Phantom measurements

In order to further validate the results of the MC simulations, measurements in clinical configurations were also done on a Rando Alderson (RA) phantom (Alderson *et al.*, 1962) filled with TLDs and equipped with various dosimeters. The RA phantom represents a 1.75 m tall and 73.5 kg male adult, without arms or legs, and is composed of multiple slices of tissue-equivalent material.

The RA phantom was placed next to the operating table as per a real procedure. The x-ray beam was centred on the patient's chest which was represented either by another RA phantom or by a polymethylmethacrylate (PMMA) slab phantom.

For each configuration, measurements were done sequentially with and without the RP device. Measurements were performed using three to four beam projections for each tested device. Those beam projections were selected because of their frequency of use (PA, LAO 30 and RAO 30) and their potential for high staff exposure (LLAT). When the beam projection was changed, all other geometrical parameters were kept constant. Additional filtration and tube voltage were automatically selected by the exposure control system of the x-ray unit.

Although it was strived to achieve identical tube output levels (P_{KA}) for similar configurations, measurement results were normalised to the P_{KA}. Efficiency of the RP device was calculated as per Equation 1.

Caps

Measurements were performed on a C-arm Philips BV unit (Philips, The Netherlands). A RA phantom and a PMMA phantom were set to represent the cardiologist and the patient (Figure 18). The distance of the RA phantom from the centre of the beam incident on the patient was 60 cm and the diameter of the FOV was 20 cm. Four projections (PA, LAO 30, LLAT and RAO 30) were selected.

Figure 18: Measurement of the efficiency of a lead-free cap on a RA phantom in a clinical set-up (LAO 30 projection).

The head of the cardiologist phantom was filled with 138 TLDs. Since the lead-free cap only protects the upper part of the head, the dosimeters in the remaining region were used to evaluate the repeatability of measurements. Four extra dosimeters were placed in two positions (near the left temple and in the middle of the forehead), both inside and outside the cap, corresponding to the TLDs used during the clinical measurements in hospital A. When the cap was not used, two TLDs were also placed on the surface of the phantom's head in order to estimate the backscatter radiation from the head, which cannot be measured by the dosimeters located outside the cap.

Masks

Measurements were performed in the same configurations as for the lead-free cap. A C-arm Philips BV unit was used with a RA phantom and a PMMA phantom representing the cardiologist and the patient, respectively. Four projections (PA, LAO 30, LLAT and RAO 30) were used.

The head of the cardiologist phantom was filled with 138 TLDs. This enabled the estimation of the dose to the brain (including cerebellum) and to the complete head region. For the evaluation of the exposure at the level of the left temple and both eye lens, three loose dosimeters were placed at each location during single exposure (Figure 19).

Figure 19: Measurement of the efficiency of a mask (model M1) on a RA phantom in a clinical set-up: 1) position of dosimeters on the left temple and the eye lens, 2) LAO 30 projection without the mask, 3).LAO 30 projection with the mask.

Drapes

A C-arm Philips BV unit was used in combination with a RA phantom and a PMMA phantom representing the cardiologist and the patient, respectively (Figure 20). Three projections (PA, LAO 30 and LLAT) were used.

As for the mask, the head of the phantom was filled with 138 TLDs. This enabled the estimation of the dose to the brain (including cerebellum) and to the complete head region, and loose dosimeters were used for the evaluation of exposure to the left temple and both eye lens (Figure 20, 1). The dose reduction efficiency for the fingers was already evaluated by means of phantom measurements using the same x-ray system in a previous work of Grabowicz et al. (Grabowicz *et al.*, 2017). The left ring finger was represented by an ISO rod phantom (ISO 2004) placed above the drape. TLDs (Radcard) were attached to the rod phantom. The results for PA, LAO30 and LAO90 projections are included for the purpose of comparison.

Figure 20: Measurement of the efficiency of a lead drape (LITE TECH, INC., USA) on a RA phantom in a clinical set-up: 1) position of dosimeters on the left temple and the eye lens, 2) LAO 30 projection without the lead drape, 3). LAO 30 projection with the lead drape.

Zero-Gravity suspended system

Irradiations were performed on a C-arm GE Innova IGS 5 unit (GE Healthcare, France). Three projections (PA, LAO 30 and LLAT) were selected. Both the cardiologist and the patient were represented by a RA phantom.

The cardiologist phantom was 70 cm away from the 20x20 cm^2 x-ray field which was centred on the patient's heart (Figure 21). The cardiologist phantom could not be placed closer to the beam centre due to the bulkiness of the ZG system. The phantom was filled with 33 MCP-N TLDs inserted into the brain and two detectors into the eye bulbs. Five eye-lens dosimeters were positioned on the face of the phantom (two on the temples, two on the eyes and one on the nasal bridge). Four Raysafe i2 dosimeters were positioned at the level of the waist, the chest, the thyroid and the left temple. These dosimeters were above the apron or directly on the phantom when the Zero Gravity was used.

Figure 21: Measurement of the efficiency of the ZG system on a RA phantom in a clinical set-up.

2.6 Statistical analysis

Descriptive statistics (mean and standard deviation or median and quartiles, depending on the observed distribution) were used to summarise the measurement results, and boxplots are used for graphical representation. Differences between study and control groups were compared using Man-Whitney U test. A p value < 0.05 was considered significant.

2.7 Device efficiency

For all simulated organs and dosimeters, the dose reduction efficiency of the RP device was calculated as the difference between the absorbed dose with the RP device (D_{RP}) and the dose without the device (the control dose, D_C), normalised to the dose without the device:

$$\frac{D_C - D_{RP}}{D_C} \qquad \text{Equation 1}$$

The efficiency was also calculated for dosimeters placed above and under the caps and the masks. To avoid confusion, it is referred to as attenuation in the rest of the report to avoid confusion, and is calculated as the difference between the absorbed above the RP device (D_A) and the dose under the device (D_U), normalised to the dose above the device:

$$\frac{D_A - D_U}{D_A} \qquad \text{Equation 2}$$

3. Results

Caps

MC

Efficiency (as per Equation 1) of the lead and lead-free caps is given in Table 6. On the whole, results obtained for the two caps are very similar. The attenuation (as per Equation 2) from the dosimeters placed above and under the protection near the left eye brow is around 89% for the lead cap and 85% for the lead-free cap. In addition, there is a potential for significant dose decrease for the brain especially at 70 cm: on average it ranges between 13% and 37% at 40 cm and 70 cm, respectively, when the head is at 0°. The efficiency is a little bit higher for LLAT projection. Moreover, efficiency for the brain is improved when the head is rotated at 30° (around 30% and 55% at 40 cm and 70 cm, respectively). However, whatever the head orientation, some parts of the brain are more protected than others (Figure 22). As expected, both caps are inefficient regarding dose reduction to the eye lens (less than 1.5%).

Table 6: Efficiency of the lead and lead-free caps for different projections at 40 cm and 70 cm. Attenuation is also reported for the dosimeters positioned close to the left eye brow. Results from MC simulations.

		70 cm					40 cm				
		PA	LAO45	RAO45	LLAT	RLAT	PA	LAO45	RAO45	LLAT	RLAT
Brain (head 0°)	Lead cap	36%	40%	32%	44%	35%	14%	15%	10%	16%	13%
	Lead free cap	35%	39%	31%	43%	33%	13%	14%	9%	15%	12%
Brain (head 30°)	Lead cap	53%	57%	51%	60%	54%	28%	32%	24%	33%	31%
	Lead free cap	51%	55%	48%	58%	51%	26%	31%	23%	32%	30%
Left eye lens (head 0°)	Lead cap	1%	1%	1%	1%	1%	1%	0%	0%	0%	0%
	Lead free cap	0%	1%	1%	0%	1%	0%	1%	0%	0%	1%
Dosimeters (head 0°) (left eyebrow)	Lead cap	88%	89%	89%	91%	90%	84%	88%	88%	89%	89%
	Lead free cap	83%	86%	84%	89%	86%	82%	85%	85%	88%	86%

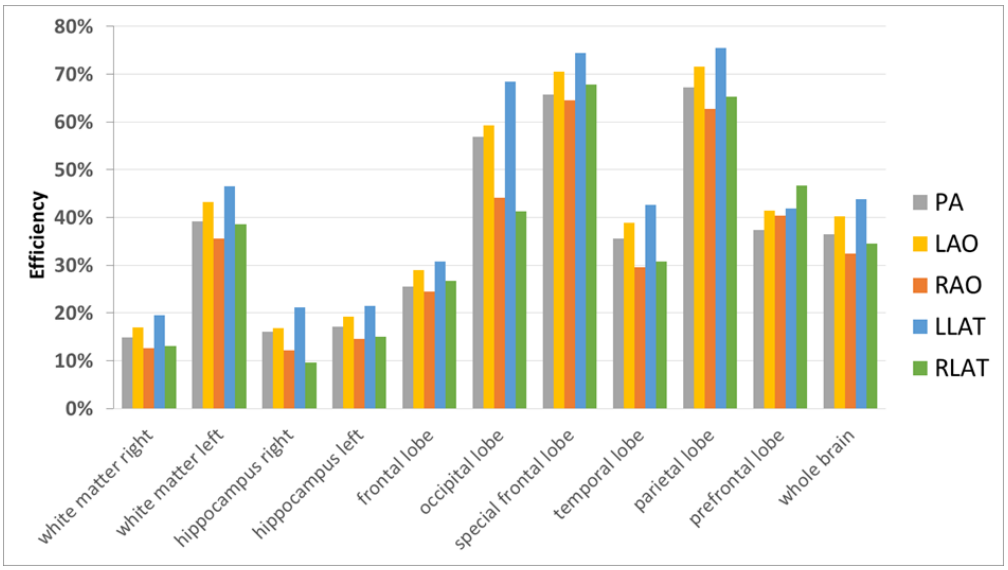

Figure 22: Efficiency for the different parts of the brain obtained for the lead cap at 70 cm (head at 0°).

Depending on the dosimeter location, the calculated cap attenuation differs considerably (Figure 23). The attenuation obtained from the dosimeters located near the left eyebrow and on the left temple is quite similar (around 88%) and does not vary much whatever the projection, the head position (0° or 30°) and the operator position (40 cm or 70 cm). By contrast, the attenuation obtained from the dosimeters located between the eyes is less than the one obtained from the two other dosimeter position and varies considerably according to the projection, the head orientation and the operator location. In particular, the mean attenuation obtained for the head at 0° over the five projections is 69% and 80% at 40 cm and 70 cm respectively. Moreover, a lower efficiency is obtained with LLAT projection for the head at 0° for both operator positions. Finally, with the head rotated at 30° the cap completely loses its efficiency especially for LAO and LLAT (values below 0) for both operator positions.

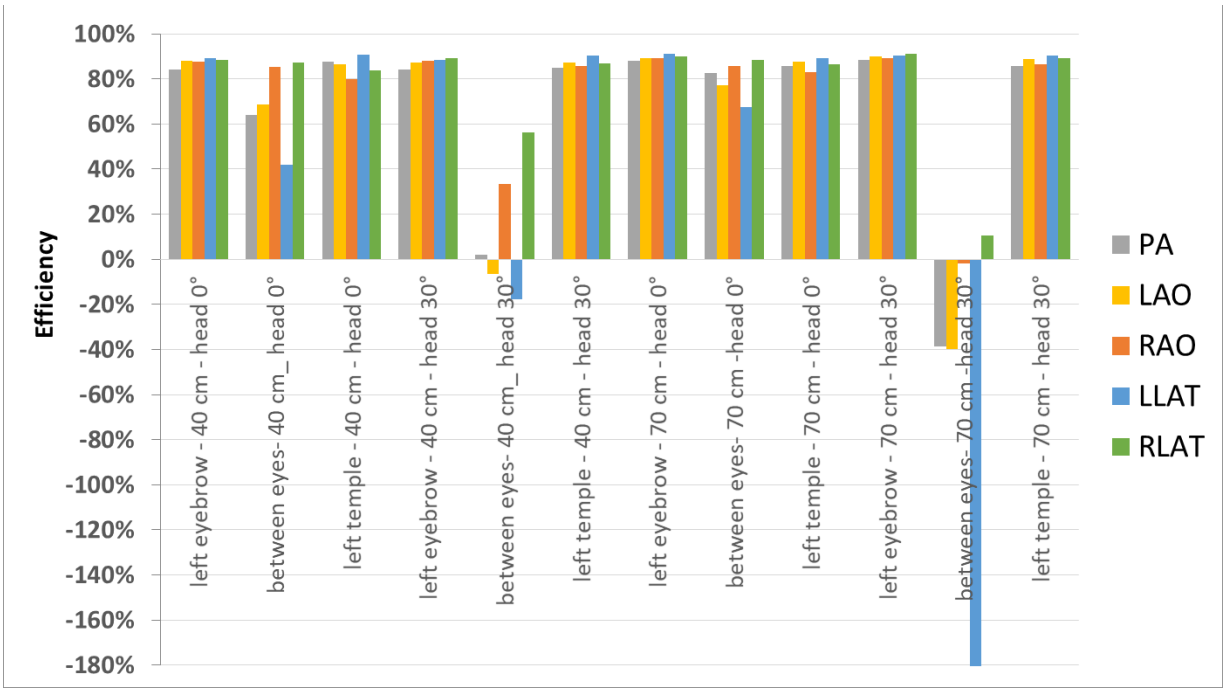

Figure 23: Lead cap efficiency obtained from the dosimeters placed above and under the cap, at 40 cm and 70 cm and for the head at 0° and 30°.

Staff

Results from measurements performed in hospital A during both phases are reported in Figure 24. During the first phase, the dosimeters were read after each single procedure. The resulting attenuation of lead-free cap varies from 0% to 70%. The average value is almost the same across the forehead and ranges from 38% for the right temple up to 44% for the left one (the standard deviation for attenuation efficiency measured in a certain position on the forehead is 0.1). The doses measured in the parts of the head which were not protected by the lead-free insert (on the top, back or in the region between both) are comparable and low, close to the lower detection limit.

The attenuation for the second phase was obtained from doses cumulated over few procedures. The average attenuation value for the middle of the forehead (on the level of eyebrows), the left eyebrow and the left temple equal 50%, 53% and 57%, respectively, while the range is 0% to 75%. Generally, attenuation coefficients are slightly larger than the ones obtained in the first phase; the latter, due to their low values below the LDL, might have been biased.

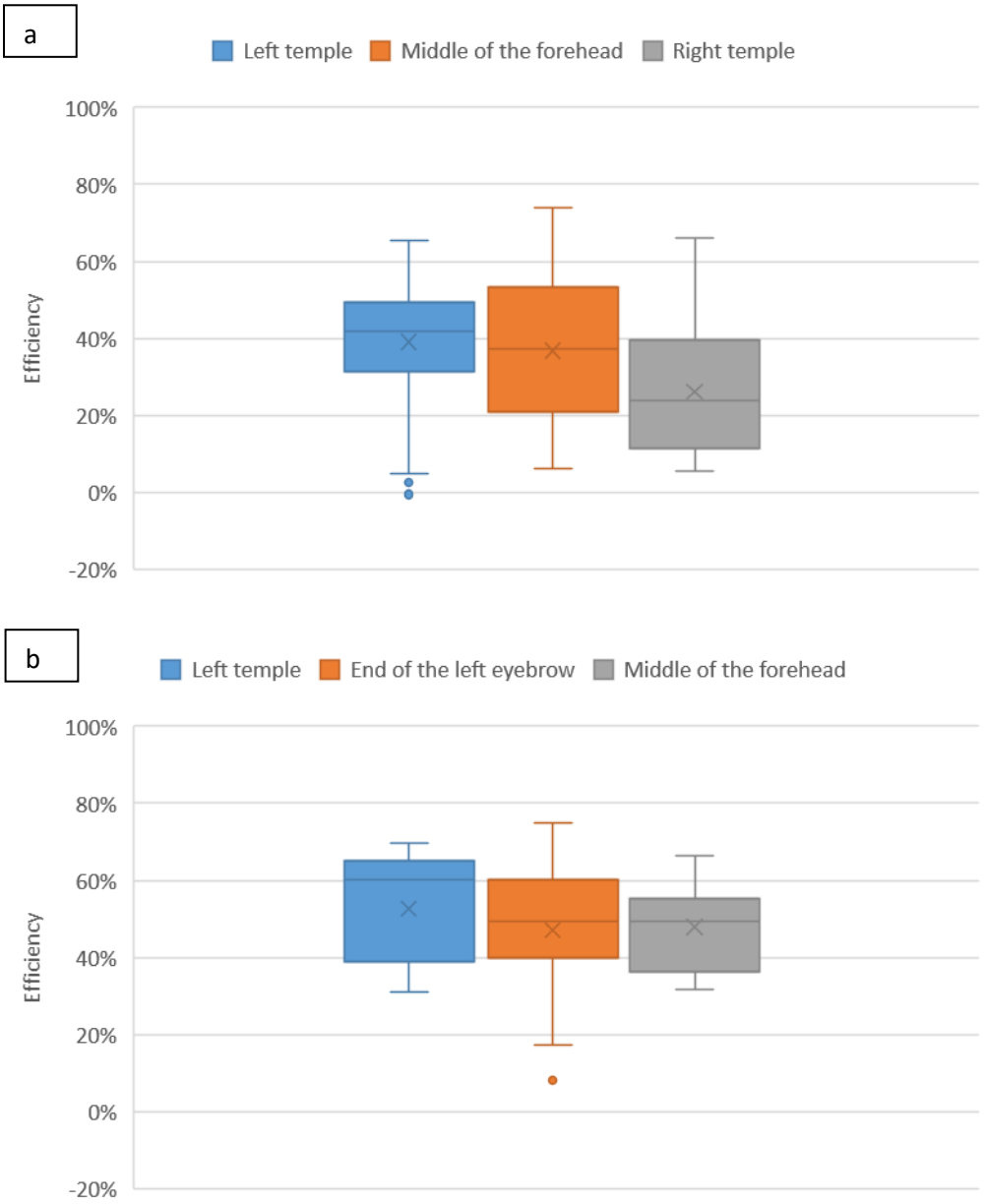

Figure 24: Lead cap efficiency: Results from staff monitoring in hospital A during the first (a) and the second phase (b)

In hospital B, where a 5-mm-thick lead cap was used, eight out of 20 measurements were below the LDL. Those dosimeters were distributed on both sides of the head, without a clear pattern. Only one dose measurement was below the LDL when the lead cap was not used. The average normalised efficiency on the left side was 53%, with values ranging from 36% to 84% and a value of -54% (i.e. dose increase). On the right side, the average normalised efficiency was 22% with values ranging from 8% to 67% and -4% and -44%.

In hospital C, all reported doses were above the LDL. The average normalised efficiency on the left side was 54%, with values ranging from 22% to 85%. The average efficiency on the right side was49%, with values ranging from 16% to 81%.

Phantom

The results of protective efficiency of the lead cap obtained from the dosimeters located inside or on the head of the phantom are presented in Table 7. For all projections the attenuation coefficients

acquire the highest values, varying from 84% to 89%, for the left temple. The lowest ones are found for the middle of the forehead. In particular, for LLAT projection the corresponding value is negative.

Table 7: Lead cap efficiency: Results from phantom measurements

	PA	LAO 30	LLAT	RAO 30
middle of the forehead	63%	79%	-11%	70%
Left eyebrow	80%	84%	76%	85%
Left temple	85%	84%	87%	89%
Top of the head covered by the cap*	30%	38%	44%	28%
Brain and cerebellum	3%	12%	10%	4%
head	3%	12%	12%	7%

*(including frontal and part of parietal lobe and the part of the skull)

The protection for the part of the head covered by the lead – free cap (including frontal lobe and part of parietal lobe and the skull) varies depending on the projection used from 28% (for RAO 30) to 44% (for LLAT). It follows from the measurements on the phantoms that the attenuation for the dose to both brain and cerebellum is relatively small. The corresponding measured maximal attenuation efficiency is 12%. The same result was obtained for the head.

Masks

MC

M1 and M2 masks attenuation obtained from the dosimeters placed at different locations above and under the mask is given in Table 8. Attenuation ranges from 72% to 90% and from 56% to 94% for M1 and M2 respectively. While attenuation for M1 is similar whatever the location of the dosimeters, a lower attenuation is observed for M2 for the dosimeters located on the right higher rim, in particular at 70 cm. However, the mean attenuation for a given distance is comparable between the two masks, around 83% and 77% for 40 cm and 70 cm respectively.

Table 8: M1 and M2 masks attenuation obtained from the dosimeters placed at different locations above and under the mask for the different projections at 40 cm and 70 cm

		40 cm						70 cm					
		PA	LAO45	RAO45	LLAT	RLAT	**Mean**	PA	LAO45	RAO45	LLAT	RLAT	**Mean**
Mask M1	Left lower rim	75%	79%	83%	86%	85%	**82%**	73%	76%	74%	81%	78%	**76%**
	Right lower rim	78%	81%	84%	85%	83%	**82%**	76%	79%	77%	84%	83%	**80%**
	Left higher rim	81%	86%	87%	90%	89%	**87%**	79%	82%	80%	86%	84%	**82%**
	Right higher rim	75%	82%	83%	86%	83%	**81%**	75%	78%	72%	81%	73%	**76%**

Mask M2	Left lower rim	88%	93%	86%	92%	89%	**90%**	77%	81%	78%	85%	82%	**81%**
	Right lower rim	83%	85%	79%	88%	81%	**83%**	76%	79%	73%	84%	74%	**77%**
	Left higher rim	92%	81%	90%	95%	93%	**90%**	81%	83%	81%	88%	86%	**84%**
	Right higher rim	82%	85%	66%	89%	67%	**78%**	65%	69%	56%	72%	64%	**65%**

M1 mask efficiency for eye lens, brain and $H_p(3)$ dosimeter for the different projections and the two distances investigated (head at 0°)are presented in Figure 25 . For all projections, a better efficiency is obtained at 70 cm compared to 40 cm. Additional calculations performed at 50 cm and 60 cm for PA projection indicate that the increase of $H_p(3)$ efficiency occurs between 60 cm and 70 cm (Table 9). Whatever the projection, M1 efficiency for eye lens is less than 2% and 8% at 40 cm and 70 cm respectively (Figure 25). Mean efficiency for the brain is around 12% at 40 cm and 43% at 70 cm. At 70 cm, efficiency for $H_p(3)$ is around 65% which is much more than efficiency for eye lens.

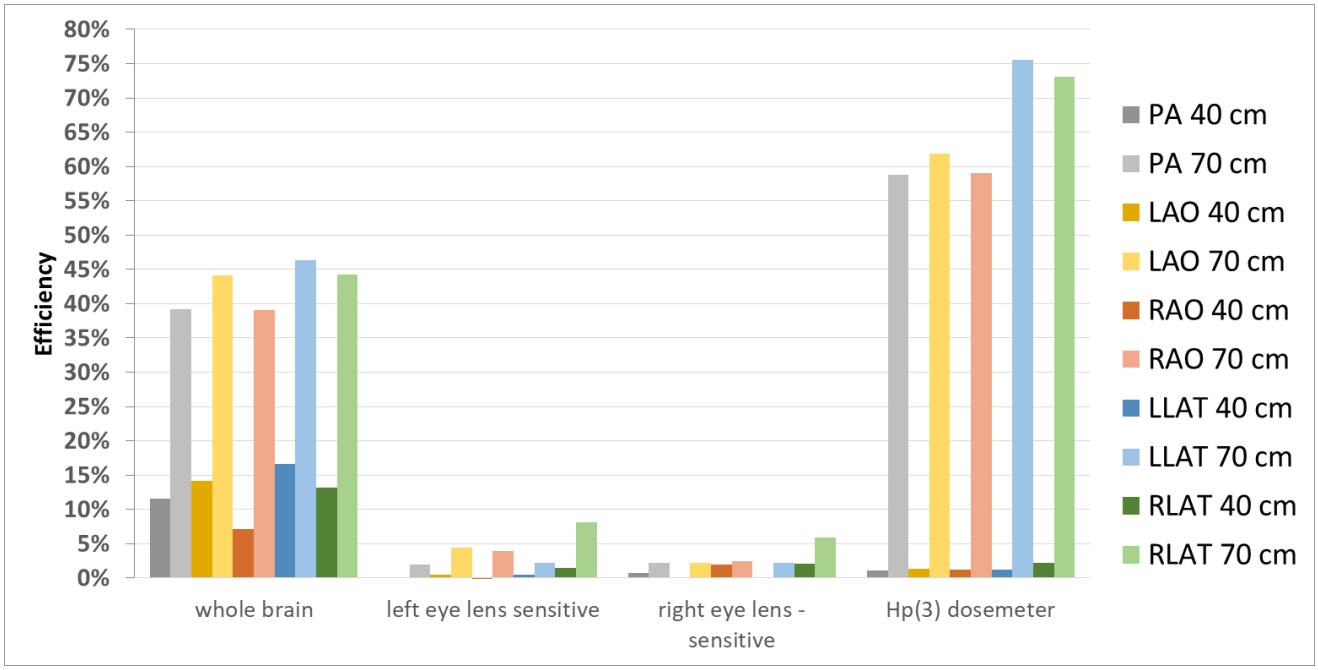

Figure 25: M1 efficiency for brain, eye lens and Hp(3) dosimeter for the different projections and the two operator positions investigated (head at 0°).

Table 9: M1 efficiency for brain, eye lens and Hp(3) dosimeter for PA projection and four operator positions (head at 0°).

	Whole brain	Left eye lens	Right eye lens	Hp(3) dosimeter
PA –40 cm	11.6%	0.1%	0.8%	1.1%
PA–50 cm	20.3%	1.2%	0.0%	3.4%
PA – 60 cm	31.6%	1.8%	1.4%	19.5%
PA – 70 cm	39.2%	1.9%	2.1%	58.8%

M1, M1L and M2 efficiency for eye lens, brain and $H_p(3)$ dosimeter for the head at 0° and 30° and the two distances investigated are presented in Figure 26. Efficiency is averaged over the five projections.

Regarding M1, no significant difference is observed between the head at 0° and the head at 30°, except for the brain efficiency which is a little bit enhanced at 40 cm when the head is rotated. M1L, which is a lengthened version of M1, is much more efficient than M1 for the brain (62%), the eye lens (64% (left) and 42% (right)) and $H_p(3)$ dosimeter (84%) at 40°cm as well as at 70 cm especially for the brain and the eye lens. Finally, with the head at 0°, M2 is very efficient for eye lens (around 70% (left) and around 55% (right)) and Hp(3) (around 60%) and to a lesser extent for the brain (around 20%) at 40 cm and 70 cm. Besides, it drops down to a few percent with the head rotated at 30° for both distances.

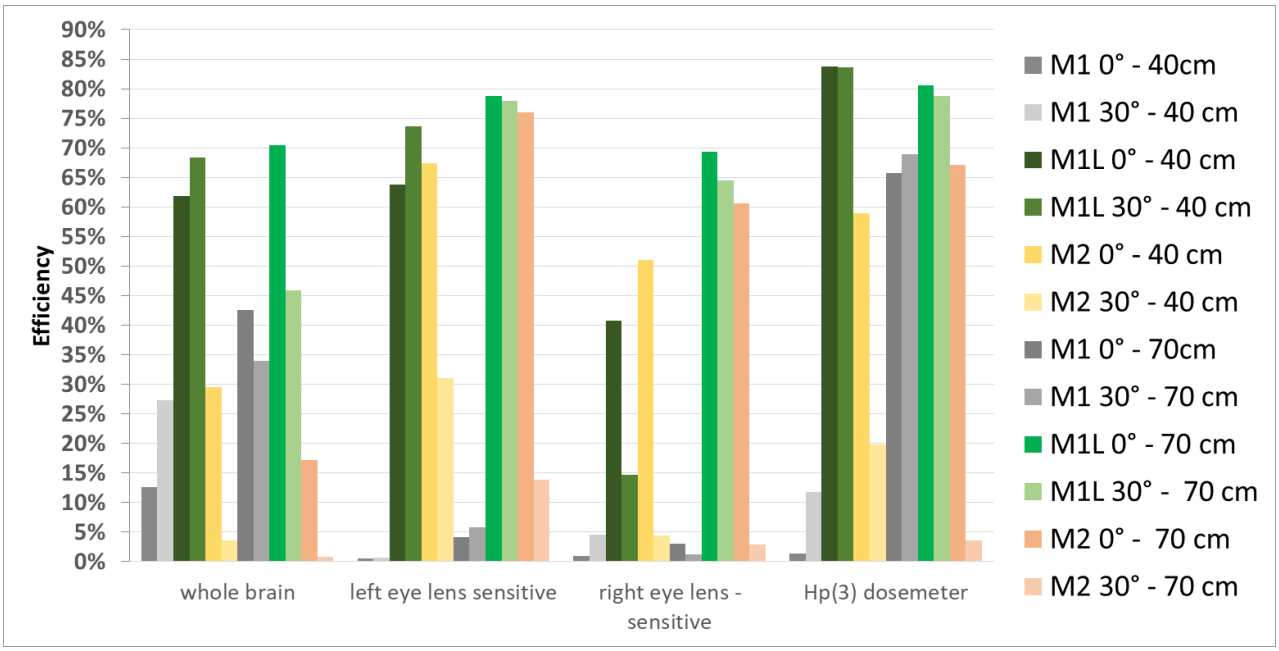

Figure 26: M1; M1L and M2 efficiency for brain, eye lens and $H_p(3)$ dosimeter for the head at 0° and 30° and the two distances investigated.

Phantom

The mean reduction efficiency, resulting from phantom measurements with M1 mask (Table 10), for the eye lens was equal or below 10% depending on the projection while for the left temple it was in the range 38% - 68%. The attenuation values for the whole brain did not exceed 17%. A similar range of protection was observed for the head (20%).

Table 10: Mask efficiency: Results from phantom measurements

Anatomical region	PA	LAO 30	LLAT	RAO 30
Brain*	33%	42%	50%	46%
Brain including cerebellum	5%	14%	17%	14%
Head	12%	15%	20%	16%
left temple	43%	38%	68%	-
left eye lens	10%	10%	0%	-

right eye lens	-	9%	-2%	-

*Including frontal lobe and part of parietal lobe and the skull

Drapes

MC

In a fixed clinical setting, the reduction to the head region was low. Different projections resulted in dose reductions around 3% on average for the brain and the eye lens (Table 11). The mean efficiency was slightly higher at 70 cm (2.9%, 3.8% and 4.4% for the brain, the left and the right eye, respectively) compared to 40 cm (1.6%, 2.3% and 2.5% for the brain, the left and the right eye, respectively). The drape was more efficient for RAO45 projections for both operator positions: for that projection, the efficiency ranged from 5.9% to 10.5%. Little difference exists between dose reduction to the eye lens ($H_p(3)$) dosimeters and to the actual eye lens.

Table 11: Efficiency for whole brain, eye lens and $H_p(3)$ dosimeter obtained for the drape at 40 cm and 70 cm (head at 0°)

	40 cm						**70 cm**					
	PA	LAO45	RAO45	LLAT	RLAT	**Mean**	PA	LAO45	RAO45	LLAT	RLAT	**Mean**
Whole brain	1.0%	0.7%	5.9%	0.2%	0.3%	**1.6%**	3.6%	2.2%	7.4%	0.5%	0.7%	**2.9%**
Left eye lens	1.4%	0.9%	8.5%	0.3%	0.3%	**2.3%**	5.3%	3.2%	9.1%	0.6%	0.8%	**3.8%**
Right eye lens	2.2%	1.8%	7.2%	0.5%	0.6%	**2.5%**	6.4%	3.1%	10.5%	0.9%	1.0%	**4.4%**
$H_p(3)$ dosimeter	1.3%	0.8%	10.1%	0.2%	0.3%	**2.5%**	4.2%	2.6%	8.1%	0.5%	0.7%	**3.2%**

As illustrated in Figure 27, dose reduction trends for specific brain regions are comparable to the trends observed for the complete brain.

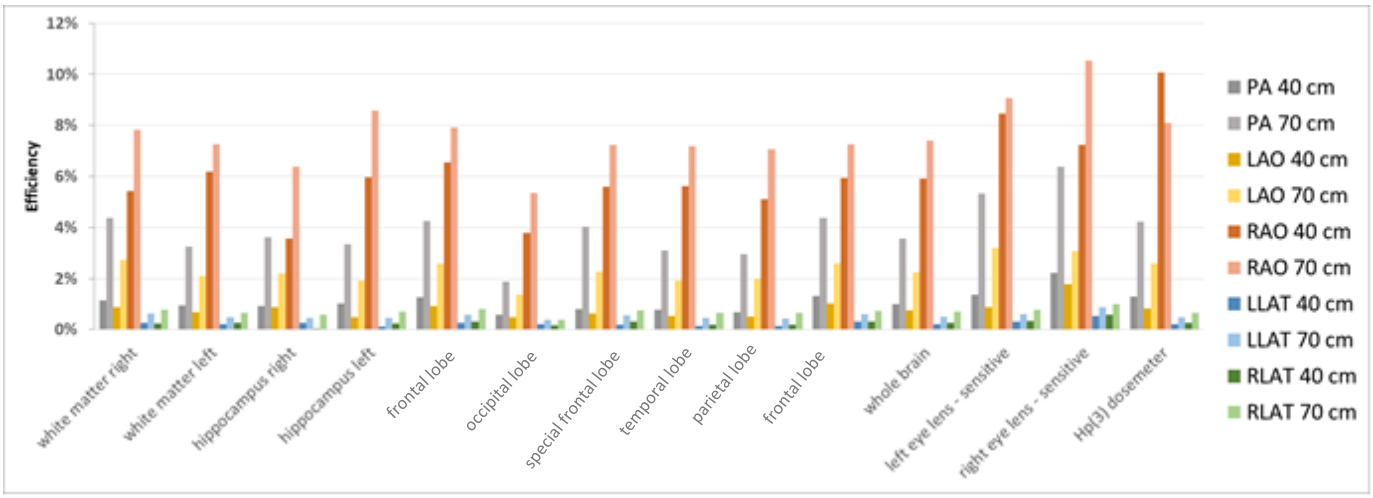

Figure 27:Efficiency for the different parts of the head, as per Figure 6, obtained for the drape at 40 cm and 70 cm.

A greater dose reduction was observed for organs situated in the direct vicinity of the drape, such as the hands and, in a lesser extent, the arms. In particular, average reduction of 62% and 30% are observed to the left and right hands, respectively, when they are directly situated above the drape

(40 cm). A decrease up to 72% and 40% is observed for the left hand in RAO45 and for the right hand in RLAT, respectively. In contrast, average reduction to the left and right hands is only 18% and 8% when the hands are further away from the drape (70 cm). Reduction to other extremities not in the close vicinity of the drape is much more limited (forearm) or inexistent (leg).

Aside from the hands, the drape also appears to decrease the dose to some organs situated in the abdomen region, although already protected by the apron, but only for right projections (RAO45 and RLAT). For instance, a dose reduction of 18% and 48% is observed for the uterus in RLAT at 40 cm and 70 cm, respectively. Absolute dose reduction, however, is small since the lead apron offers an important dose reduction as underlined by the results in Table 15.

Table 12: Dose reduction efficiency of the drape for other organs at 40 cm and 70 cm.

	40 cm						70 cm					
	PA	LAO45	RAO45	LLAT	RLAT	**Mean**	PA	LAO45	RAO45	LLAT	RLAT	**Mean**
Right hand	30%	30%	37%	12%	40%	30%	8%	10%	9%	6%	7%	8%
Left hand	64%	68%	72%	36%	71%	62%	21%	16%	22%	9%	24%	18%
Right forearm	19%	18%	24%	3%	27%	18%	12%	16%	20%	9%	13%	14%
Left forearm	4%	3%	10%	0%	8%	5%	18%	19%	26%	3%	24%	18%
Right leg	0%	0%	0%	0%	0%	0%	0%	0%	0%	0%	0%	0%
Left leg	0%	0%	0%	0%	0%	0%	0%	0%	0%	0%	0%	0%
Hp(10) above apron Left up	3%	3%	9%	1%	1%	3%	7%	6%	15%	1%	5%	7%
Gonads*	1%	1%	1%	1%	3%	1%	3%	2%	2%	2%	7%	3%
Lungs	2%	1%	6%	0%	1%	2%	3%	2%	12%	0%	2%	4%
Stomach wall	1%	1%	2%	0%	4%	2%	14%	8%	20%	2%	19%	12%
Uterus	2%	2%	2%	1%	18%	5%	9%	5%	8%	2%	48%	14%
Bladder wall	2%	2%	2%	0%	17%	5%	6%	5%	6%	5%	28%	10%
Liver	7%	4%	13%	1%	9%	7%	14%	10%	28%	1%	14%	13%
Heart	2%	2%	4%	0%	1%	2%	6%	4%	17%	1%	5%	7%
Kidneys	1%	1%	3%	0%	12%	4%	10%	3%	15%	1%	23%	10%

*Gonads are testes and ovaries

Varying the position of the drape as depicted in Figure 11 (only tested in PA with the cardiologist at 70 cm from the x-ray field) could have a strong influence on the dose reduction. Moving the drape 5 cm towards the patient head reduced the left eye dose by 10% and the dose to organs in the abdomen region up to 20%, but this had no effect on the hand exposure. Moving the drape away from the x-ray field had an opposite effect, while lateral movement had no effect as long as the patient side was completely covered. The three additional designs had mostly no influence but on the hand dose. The design offering a wider coverage of the patient directly under the hands were more efficient and could decrease further the dose to the right hand by 10%. In contrast, design decreasing the coverage of the patient under the hand resulted in an increased hand dose (up to 25%).

Phantom

The mean reduction efficiency, resulting from phantom measurements with a lead drape on the patient abdomen (Table 13), was equal or below 13% for the eye lenses, depending on the projection. A comparable range was observed for the left temple. No meaningful dose reduction was observed at

the level of the head or brain (no more than 3% dose reduction. As for the protection of the left finger, this issue was studied by Grabowicz et al. in 2017. The highest dose attenuation (68%) was observed in the PA projection. However, it decreased significantly with increasing angle until there was no effect at LLAT.

Table 13: Lead drape efficiency: Results from phantom measurements

Anatomical region	PA	**LAO 30**	LLAT
Brain*	-3%	-1%	2%
Brain including cerebellum	-1%	3%	-1%
Head	-2%	5%	3%
left temple	12%	9%	9%
left eye lens	3%	7%	13%
right eye lens	10%	3%	0%
left finger**	68%	17%	0%

*Including frontal lobe and part of parietal lobe and the skull

**from Grabowicz et al. 2017; distance from the operator to the centre of the x-ray field was 40 cm in contrary to the remaining anatomical regions where it was 60 cm.

Staff

In Hospital D (Figure 28), a statistically significant difference ($p<0.05$) was observed between the doses measured at all locations. The dose reduction was important: 38% and 18% at the level of the left and right fingers (ring dosimeters), respectively, and 50% and 52% at the WB dosimeter (above the lead apron) and the eye lens dosimeter, respectively (Table 14).

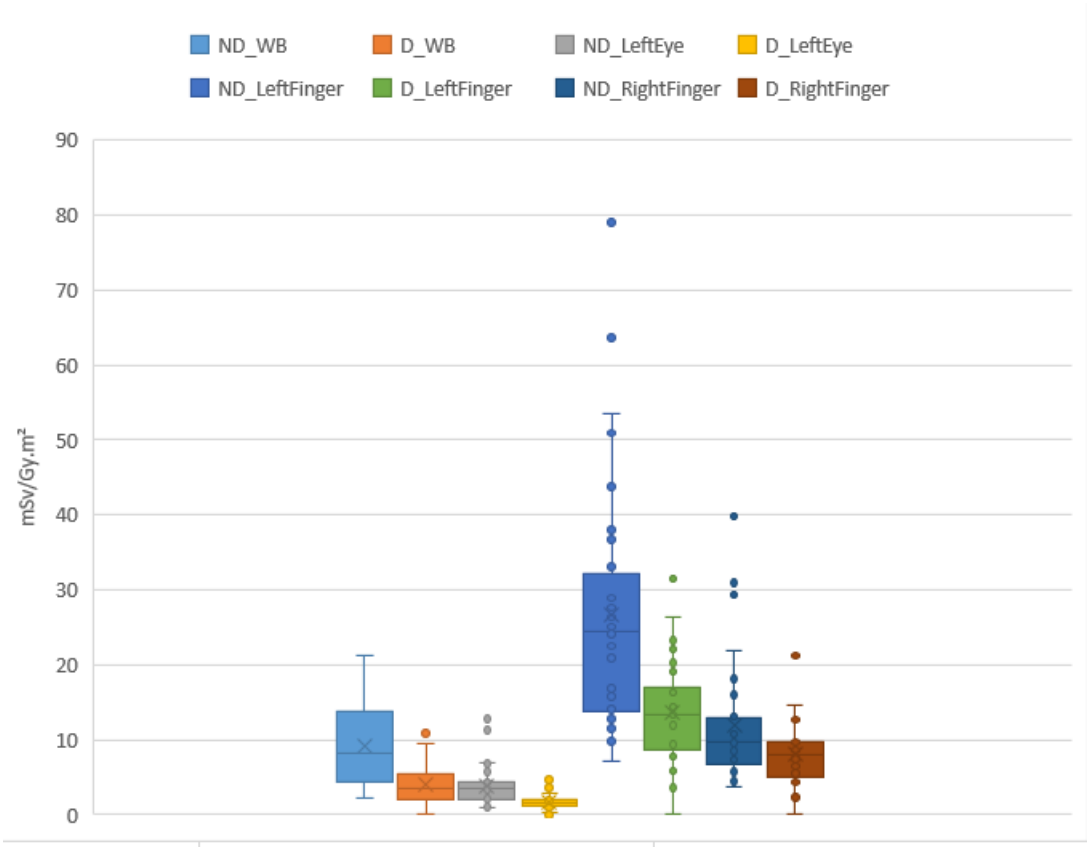

Figure 28: Lead-free drape efficiency: dose measurements at three different dosimeter locations with (D_) and without the drape (ND_) in hospital D.

In Hospital E (Figure 29), a statistically significant difference ($p<0.05$) was only observed at the level of the left finger and the whole body dosimeter worn on the chest, with reduction of 22% and 34%, respectively.

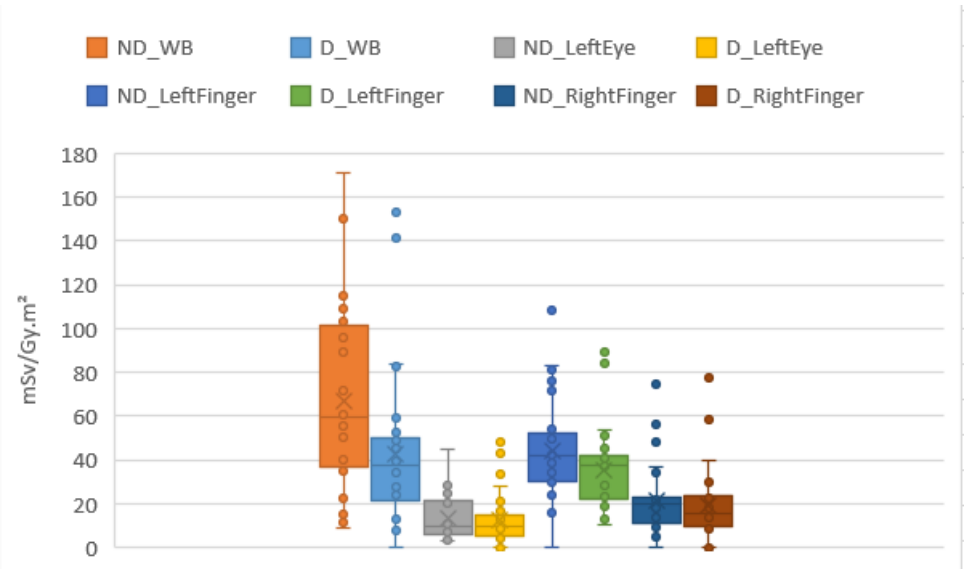

Figure 29: Lead-free drape efficiency: dose measurements at three different dosimeter locations with (D_) and without the drape (ND_) in hospital E

Table 14: Average lead-free and lead drape efficiency from staff measurements in hospital D and E, respectively

Average reduction	Whole Body	Left Eye	Left Finger	Right Finger
Hospital D	52%	50%	38%	18%
Hospital E	34%	-3%	22%	9%

Aprons

MC

Efficiency obtained for the lead and lead-free aprons for the different projections at 40 cm and 70 cm is given in Table 15. The lead-free aprons show no noticeable difference compared to lead aprons, irrespective of the simulation conditions. For the lead apron, effective dose reduction is 81 % at 70 cm and 92 % at 40 cm. These reductions are respectively 77 % and 89 % for the first lead-free apron and 79 % and 91 % for the second. The dose reduction obtained for the dosimeter placed under the apron on the phantom torso is close to the effective dose reduction. The mean relative difference between the value obtained from the dosimeters and the effective dose variation is 3.5% for the lead apron and 6% for the lead-free aprons. However, in some cases, this difference changes drastically. For instance, for LLAT at 70 cm, the dose reduction obtained for the dosimeter placed under the apron on the phantom torso is around 33% for the three aprons whereas it is around 79% for the effective dose. For the three aprons, the larger the distance is, the lower the efficiency is. Regarding the effective dose, the mean efficiency obtained with the lead apron is 81 % at 70 cm and 92 % at 40 cm. These values are respectively 77 % and 89% for the first lead-free apron and 79 % and 91 % for the second lead free apron. However, the apron efficiency decreases only for some organs like lungs, oesophagus, brain and heart (Table 16).

Table 15: Efficiency of the lead and lead-free aprons to reduce the effective dose (E) and the dose at the chest dosimeter for the different projections at 40 cm and 70 cm

		70 cm					40 cm				
		PA	LAO45	RAO45	LLAT	RLAT	PA	LAO45	RAO45	LLAT	RLAT
LA	E	82%	83%	84%	81%	75%	93%	94%	96%	92%	86%
	WB dosim	86%	81%	91%	34%	93%	93%	93%	98%	85%	96%
LFA 1	E	79%	80%	81%	77%	71%	90%	91%	92%	90%	82%
	WB dosim	84%	79%	90%	31%	91%	91%	92%	97%	80%	95%
LFA 2	E	80%	81%	82%	78%	73%	92%	92%	94%	92%	84%
	WB dosim	87%	79%	90%	33%	92%	92%	92%	98%	92%	96%

Table 16: Comparison of the lead apron efficiency at 40 cm and 70 cm for some organs in PA projection

	Efficiency 70 cm	Efficiency 40 cm	Efficiency at 40 cm / 70 cm
Colon	97.0%	98.0%	1.01
Lungs	**47.0%**	**74.8%**	**1.59**
Stomach	91.6%	95.4%	1.04

Breast	95.6%	97.4%	1.02
Gonads	99.5%	99.7%	1.00
Bladder	98.9%	98.9%	1.00
Oesophagus	**63.5%**	**83.1%**	**1.31**
Liver	92.6%	96.8%	1.05
Brain	**4.0%**	**29.6%**	**7.40**
Salivary glands	**19.0%**	**48.6%**	**2.55**
Intestine	97.3%	98.0%	1.01
Heart	**72.4%**	**88.7%**	**1.23**
Kidneys	95.1%	96.5%	1.01
Prostate	98.7%	98.7%	1.00
Spleen	81.4%	88.2%	1.08

Staff

Comparison of the ratios of the WB doses measured above and underneath the aprons are reported in Figure 30. The average (median) attenuation was 14% (2%) higher when a lead-free or a light lead apron was used compared to a conventional lead apron. The difference was significant ($p = 0.017$). The average dose measured above the lead aprons was 16% higher but not significantly different ($p = 0.38$) than the dose measured above other types of aprons. In addition, the average dose measured underneath the lead aprons was significantly higher (29% higher, $p = 0.007$).

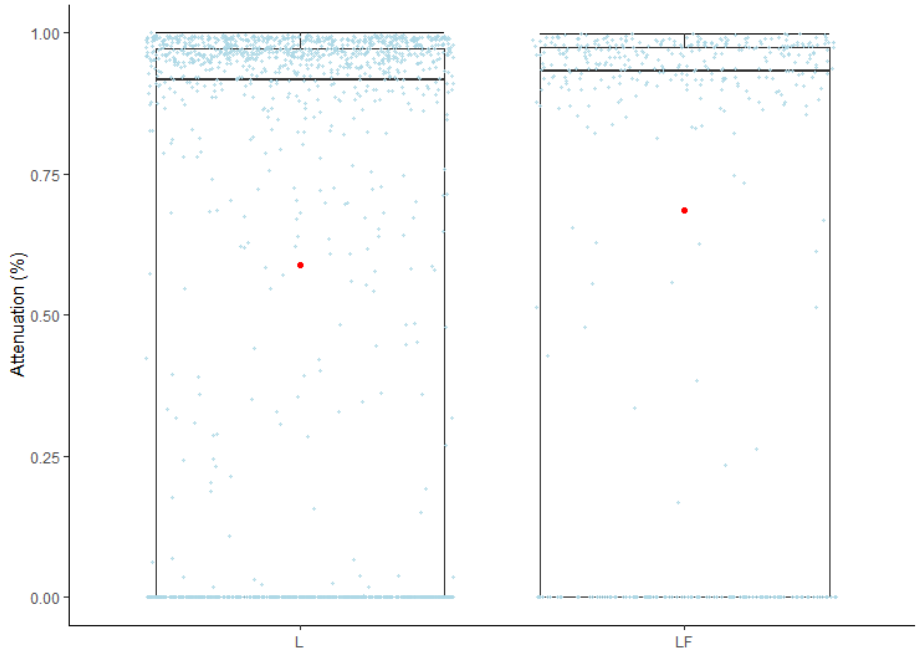

Figure 30: Boxplots of attenuation of lead-free and light lead aprons (LF) and lead aprons (L)from staff monitoring in hospitals F, G and H. Individual attenuation measurements are reported in light blue; average attenuation is reported in red.

Both for the lead apron and the lead-free or light lead apron, the number of WB measurements inferior to the LDL was important. For the lead-free or light lead apron, 26% and 60% of the measurement above and under the apron was inferior to the LDL, respectively. For the lead apron, 35% and 54% of the measurement above and under the apron was inferior to the LDL, respectively

Zero-Gravity suspended system

MC

Results obtained for the ZG are presented in Figure 31 and Table 17. Different projections resulted in average dose reduction of at least 90% for all the organs in the head and neck region (Figure 31); while dose reductions were also observed for organs normally covered by the apron (Table 17), with average dose reduction ranging from 23% to 81%. Negative dose reduction (dose increase) was also observed for the left lung and the stomach.

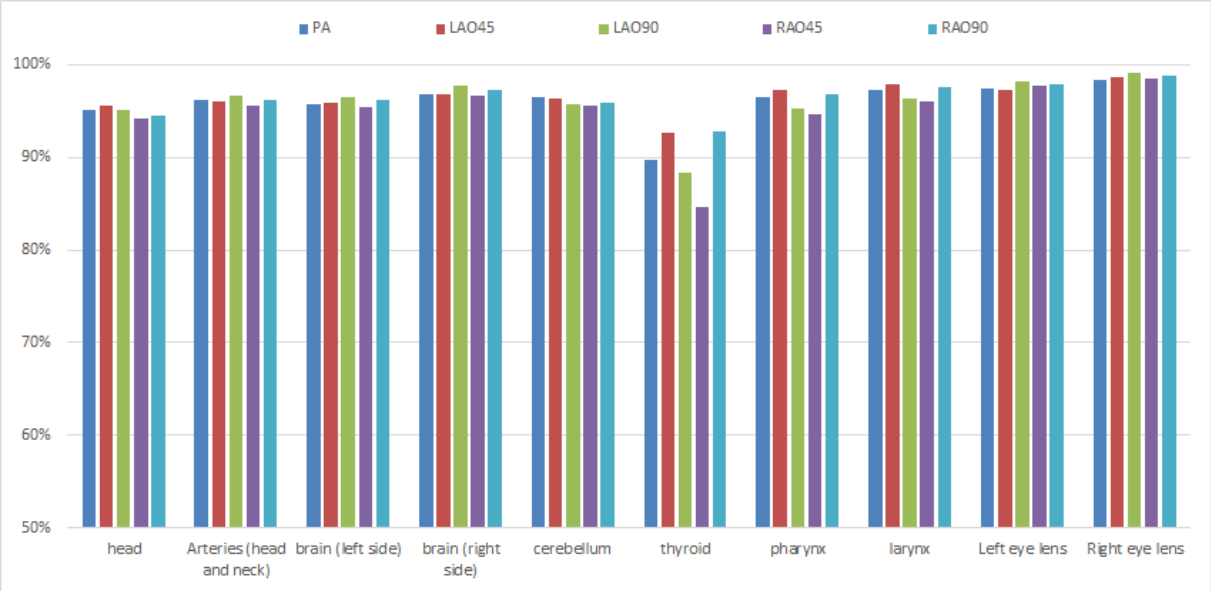

Figure 31: Reduction efficiency of ZG to various organs in the head region. Results from MC simulation in different configurations

Table 17: Efficiency of ZG system for various projections at 70 cm from the primary beam: results of MC simulations

Tissue	PA	LAO45	LLAT	RAO45	RLAT
Left lung	40%	41%	46%	5%	-18%
Right lung	79%	80%	83%	73%	69%
Stomach	71%	77%	76%	66%	-18%
Large intestine	90%	88%	88%	90%	48%
Heart	73%	73%	75%	63%	60%
Brain (left)	96%	96%	97%	95%	96%
Brain (right)	97%	97%	98%	97%	97%
Thyroid	90%	94%	88%	85%	93%
Testes	65%	61%	55%	81%	76%
Left eye lens	97%	97%	98%	98%	98%
Right eye lens	98%	99%	99%	99%	99%

Staff

Results from dose measurements with and without the ZG at the level of the chest, the left eye, the left upper arm and both ring fingers in hospital I are reported in Figure 32. Only five WB and three right finger dose measurements out of 25 were above the LDL when the ZG was used. Only three WB and ten right finger measurements were below the LDL when the ZG was not used. For other dosimeter locations, the proportion lower than the LDL could be neglected and significant dose reduction of 85%, 82% and 44% were observed at the level of the left eye, upper arm and ring finger, respectively.

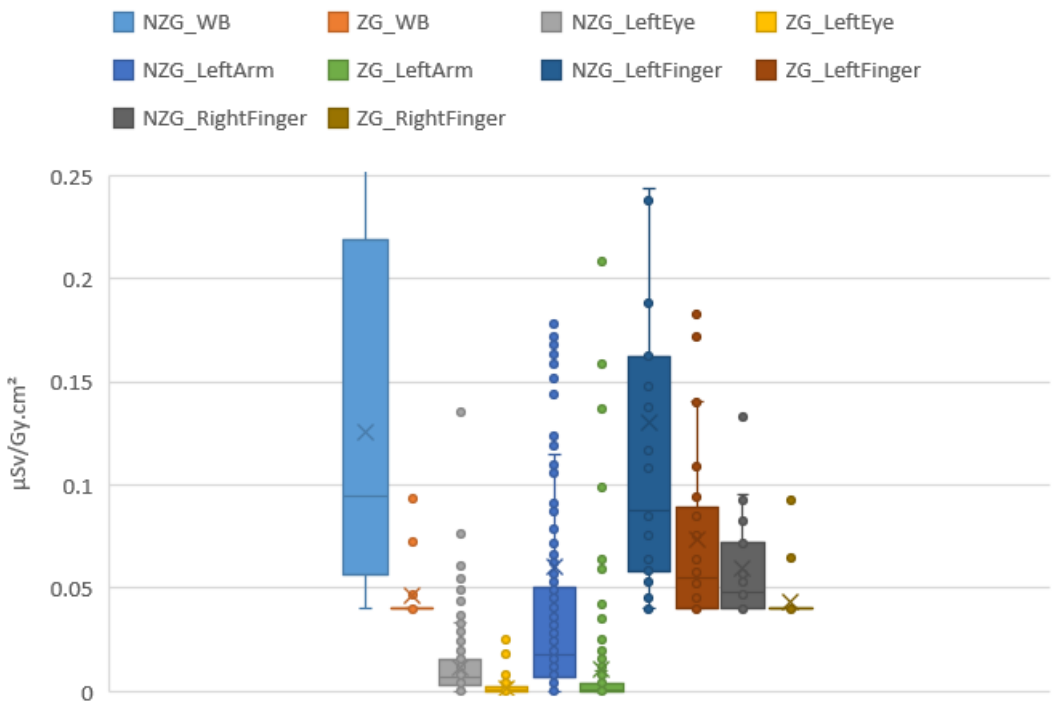

Figure 32 : ZG system efficiency: Results from staff monitoring at the level of the chest, the left eye, the left upper arm and both ring fingers in hospital I.

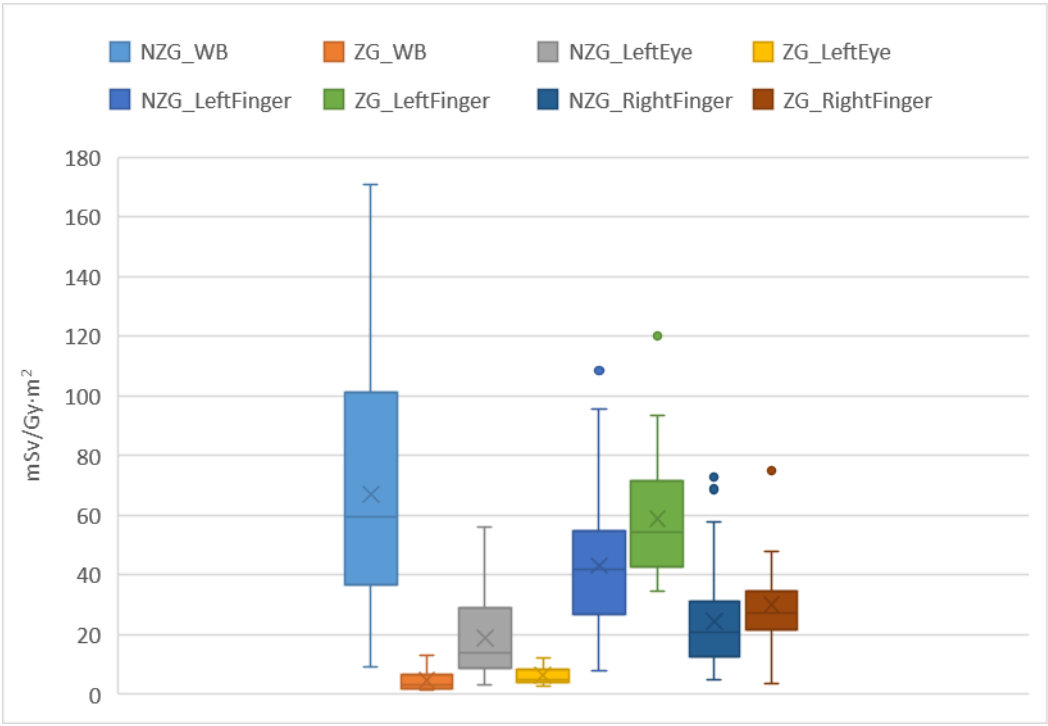

Figure 33: ZG system efficiency: Results from staff monitoring at the level of the chest, the left eye and both ring fingers in hospital K.

For all measurements performed in hospital J, where the ablation procedures were performed, all reported doses were below the LDL when the ZG system was used. In hospital K, the statistically significant reduction of 93% and 67% for eye lens and whole body (both protected with the ZG system), respectively, has been observed. It should be noted that only eight doses measured on the chest exceeded the LDL. In contrast, the exposure for the ring finger of both hands increased considerably

as compared to those resulting in the procedures performed without ZG system but with the ceiling suspended lead shield instead.

Table 18: ZG system efficiency: average dose reduction from staff monitoring in hospitals I and K. Negative values are an increase in the observed dose. Dose reduction in hospital J could not be calculated since all doses were below the LDL when the ZG system was used.

	WB	Eye lens left	Finger left	Finger Right
Hospital I	Not calculable	85%	44%	Not calculable
Hospital K	93%	67%	-36%	-23%

Phantom

The dose reduction averaged over the detectors inserted into the phantom brain was between 65% and 94% depending on the projection. The average dose reduction was slightly higher for dosimeters on the left side of the brain (86%) compared to the right side (76%), but the absolute dose to the right side of the brain was lower compared to the left side: When the ZG was not used, the right side of the brain received doses on average 53% lower than the left side.

The dose reduction to the left and right eye were between 75% and 96%. Comparable trends were observed for the dosimeters positioned on the phantom face. Since no dose was detected at the level of the waist, chest and thyroid when the Zero-Gravity system was used, the LDL was used instead (1 µGy). The dose reduction at the level of the waist and chest were virtually 100% (>99.7%); the reduction at the thyroid level was between 88% and 99%.

Table 19: Zero Gravity efficiency: Results from phantom measurements

Anatomical region	PA	LAO 30	LLAT
Brain including cerebellum	65%	94%	89%
Left temple	91%	99%	97%
Left eye lens	84%	96%	95%
Right eye lens	75%	92%	92%
Thyroid	88%	91%	99%
Chest	100%	100%	100%
Waist	100%	100%	100%

4. Discussion

Caps

From MC simulations, an average cap attenuation of 86% is obtained from the dosimeters positioned directly above and under the lead and lead-free caps. This is in agreement with the 85% obtained by Uthoff et al. (2013) from measurements on staff and with the attenuation of 81% and 86% obtained from phantom measurements at the left eyebrow and left temple respectively. The reduction level, however, could be lower (around 50% on average) in clinical conditions from dosimeters worn above and below a lead-free cap by medical staff as determined in this project.

The cap efficiency obtained from the dosimeters located on the middle of the forehead is less than the one obtained from the two other locations (left eyebrow and left temple) for both simulations and phantom measurements. This was not observed for clinical measurements in hospital A, with comparable efficiency at the three locations. In hospitals B and C, there was also no clear pattern visible in the attenuation with respect to the dosimeter position. The average attenuation was also lower than in MC simulations. This is likely explained because the cardiologists rotate their head towards the x-ray source during a real practice, while only fixed head orientations were simulated and measured on the phantom. The position of the screen monitor is a determining factor for the head orientation during real procedures. For the middle of the forehead, the efficiency obtained for LLAT projection by means of phantom measurements and by simulations with the head rotated at 30° was below 0. That means that the dose received by the dosimeter below the cap exceeds the one received by the dosimeter above the cap. This suggests that the radiations which reach the dosimeter may come from underneath the cap or may pass through the dosimeter located inside the cap before passing through the dosimeter outside. For the first hypothesis, it could be due to the fact that the cap does not fit perfectly the head of both physical and numerical phantoms while for the second one it suggests that radiations come from the left side or the back of the head.

In our simulation study, lead and lead-free caps have a potential for significant dose decrease to the brain (up to more than 35%). However, this strongly depends on the relative position of the physician with respect to the primary x-ray field: when the head was perpendicular to the patient, the average reduction was only about 13% at 40 cm whereas it was 37% at 70 cm. This is in agreement with Silva et al. (2017) who calculated an average dose reduction to the brain between 6% and 15%. This is also the same magnitude as the 7% efficiency obtained by means of phantom measurements with TLD and the 3.3% efficiency obtained by Fetterly et al. (2017) thanks to measurements with radiochromic films in an anthropomorphic phantom.

The MC simulations also showed that attenuation calculated from dosimeters located directly above and under the caps is a poor estimator of the brain protection. Indeed the attenuation derived from the dosimeters (more than 80% on average) severely overestimated the dose reduction in most configurations (on average between 13% and 37% at 40 cm and 70 cm, respectively, when the head was perpendicular to the patient). This is in agreement with Silva et al. (2017) who reported that no dosimeters placed under a cap was appropriate to estimate the brain dose reduction because, on average, only 5% of the brain exposure penetrated the head through the forehead when the physician was at 40 cm from the x-ray field.

Masks

Mask attenuation assessed by means of MC simulations is very high (82%) and similar whatever the projections. This attenuation is obtained from dosimeters placed above and below the mask itself and is not representative of the dose reduction (efficiency) for the organs and tissues located in the head. Indeed, the path of all the radiations which reach the dosimeters placed below the mask passes

through the mask and are thus attenuated. However, the path of some radiations reaching the organs located in the head with M1 does not cross the mask. As a matter of fact, the efficiency for the eye lens is very low either by Monte Carlo simulation (less than 8%) or by phantom measurements (below 10%). This suggests that most of the radiations reaching the eye when wearing M1 do not pass through the mask and thus are not attenuated. A better protection of the eye lens is obtained with M1L which is a lengthened version of M1. Therefore, radiations reaching the eye lens with M1 may come from underneath the mask. This is also confirmed, on one hand, by enhanced eye lens efficiency obtained with M2 which is also long, and on the other hand, by the higher eye lens efficiency obtained with M1 at 70 cm compared to 40 cm. At larger distances, a smaller proportion of radiation comes from underneath the mask.

Regarding dose reduction to the brain with the head at 0°, it is better with M1L at the two distances followed by M2 and then M1 at 40 cm and the contrary at 70 cm. Once again, these differences can be explained by the length and the shape of the masks. Lengthier masks are more efficient at shorter distances. However, when the distance from the source increases, M2 loses its efficiency due to its particular shape on the sides. This is even more noticeable when the head is rotated at 30° where its efficiency drops down to a few percent.

From MC simulations, $H_p(3)$ dosimeter dose decrease seems not representative of eye lens dose decrease in particular for the short mask M1 at 70 cm and would lead to an underestimation of the real eye lens dose. Similar findings are obtained with phantom measurements: Hp(3) efficiency ranges from 33% to 50% while eye lens efficiency is less than 10%. The location of $H_p(3)$ dosimeter could explain this difference: it is located on the left temple closer to the mask surface than the left eye. The additional calculations performed with the operator at 50 cm and 60 cm with M1 indicate that the dose reduction to $H_p(3)$ dosimeter increases between 60 cm and 70 cm. This suggests that between these two distances, the majority of the radiation which so far reached the dosimeter from underneath the mask come now through the mask.

Finally, comparable efficiencies (around 40%) are obtained with M1 mask for the whole brain for both simulations and phantoms measurements.

To compare the reduction efficiency of the mask and the lead-free cap as per the phantom measurements, the relevant efficiency for the part of the head normally covered by the lead – free cap were calculated for the mask. For the mask the corresponding maximal value is 50% for the LLAT projection while the minimal one equals 33% for PA.

It follows from the measurements on the phantoms that the attenuation for the dose to both brain and cerebellum is slightly higher than for the lead-free cap (12%). For the mask the measured maximal attenuation efficiency is 17%. A similar result was obtained for the complete head region (21%).

Drape

From measurements on the staff and MC simulations, a lead-free or lead drape positioned on the patient appeared to be an efficient solution to reduce the dose to the left hand and, possibly, to the right hand.

From simulations, a greater dose reduction was found when the hands were directly above the drape. The dose reduction to other locations such as the brain, the eye and the WB dosimeter, however, was very low to inexistent. Phantom measurements confirmed these results (from the present study and from Grabowicz et al. (2017)), except for the WB dose which was not measured. In contrast, clinical measurements on the staff showed significant reduction to the WB dosimeter in both participating hospitals (34% and 52% in hospitals E and D) and to the left eye in only one hospital (50% in hospital

D). The ceiling suspended-screen was used during the clinical procedures but not in the simulation models. This could partially explain such a difference. However, it is unlikely to explain it completely because the drape had very little to no effect on the WB dosimeters in the simulations. This should be further investigated.

MC simulations also showed the importance of the projections and the drape position on the efficiency. The drape was more efficient when it was closer to the primary beam (without interfering with it) and covering the side of the patient close to the cardiologist.

The considerable difference in dose reduction efficiency between the clinical measurements (at the level of the eye lens) themselves on one side, and between the hospital measurements and the MC simulation on the other side is surprising; although, such discrepancies had already been reported in the literature about use of lead or lead-free drape. Different drape models were used in both hospitals and for the simulations; however, MC simulations showed that the design had little influence as long as the side of the drape did cover the right side of the patient, including the table. In any case, this clearly indicates a considerable effect from the local practice which can strongly influence the efficiency of the drape (e.g. use of different projections and drape position, position of the screen monitor, etc.).

Effective doses were calculated using MC simulations. However, there are not presented because they merely reflect the dose reduction to the hands and forearms, the doses to other sensitive organs being identical whether a drape is used or not.

Apron

For WB dosimeters, comparable attenuations are obtained for lead and lead-free aprons by means of staff measurements as well as by numerical simulations. This is not in agreement with the study of Schlattl et al. (2007) who, from MC calculations of air kerma below an apron in a broad primary beam, reported that the shielding capability of lead-free materials composed of Sn and Sn/Bi is much lower than that of lead. This was attributed to the high proportion of low-energy photons created by fluorescence in tin. However, as several parameters are different between our study and the one of Schlattl et al. (2007) (primary beam versus scattered beam, Sn/Bi versus Sb/Bi, kV and filtration, etc.), comparison of the findings is not straightforward. Effective dose reductions obtained from our MC simulations are also quite similar for lead and lead-free aprons. The reduction is around 3% less with the lead-free aprons. Schlattl et al. (2007) reported around 3% effective dose increase with tin/bismuth shielding at 75 kV compared to lead shielding. This moderate increase, compared to the one observed for air kerma by the same authors, was attributed to the fact that low-energy photons created by fluorescence cannot penetrate deeply into the body. Therefore, they observed a distinctive dose increase only in organs located very superficially, as glandular breast tissue for instance.

The decrease of efficiency, noticed with numerical simulations, when the distance from the source increases may be attributed to two factors. On one hand, moving away from the source, the shadow mask created by the apron on the head and neck region could be reduced. This would explain the lower efficiency obtained for the brain and the thyroid at 70 cm. On the other hand, there are some holes in the apron in order to pass the arms. They are not wide, but their height can reach 20 cm; thus when the distance from the source increases, the trunk and organs like the heart are more exposed because not protected by the apron due to these holes. It should also be kept in mind that the absolute organ dose usually decreases further away from the primary x-ray field. For instance, the dose to the organs included in the effective dose calculations decreases on average by about 60% at 70 cm with respect to 40 cm.

Except for LLAT at 70 cm, there is a good agreement between the reduction for the dosimeters and the effective dose. Therefore, the dose reduction to the dosimeters is a good approximation of the apron efficiency for the effective dose.

The conclusions from the MC simulations did not conflict with the study of the monthly dose monitoring above and underneath the apron and their average attenuation. On average, the attenuation was slightly (14%) higher when a lead-free or a light lead apron was used compared to when a lead apron was used. This might indicate that lead-free or light lead aprons are nearly as efficient as a lead apron and, therefore, are acceptable substitutes. Obviously, this is only indirect evidence and results are affected by the important number of measurements inferior to the LDL for both types of aprons and dosimeter position, as well as the relatively small number of cardiologists monitored and.

The dose reduction obtained for the dosimeter placed under the apron on the phantom torso is close to the effective dose reduction. This is relevant in routine monitoring when a single dosimeter under the apron is used to estimate the effective dose, but not when double dosimetry is used.

Zero-Gravity suspended system

As demonstrated by MC simulations and measurements (both on staff and on phantom), the ZG is at least equivalent to the lead and lead-free aprons for the organs and dosimeters usually covered by the latter. In addition, MC simulations showed at least 90% dose reduction to the sensitive organs in the head region. In contrast with the mask and the cap which partially cover the head, the ZG efficiency is rather homogenous for all tissue and organs in the brain region.

Reduction to the eye lens dose ranges from 83% to more than 95% depending on the projection. This is in agreement with the eye lens dose measurements in hospital I and K, and also with the study of Savage et al. (Savage *et al.*, 2013) who reported 94% reduction during various types of interventional procedures and more effective than the 50% dose decrease to the eye lens reported by Haussen et al (Haussen *et al.*, 2016) during interventional neuroprocedures. Difference in dose might be due to an incorrect placement of the ZG face shield, letting the eye partially exposed. The simulations are also consistent with the validation measurements performed on an anthropomorphic phantom showing dose reduction to the brain and eye lens from 65% up to 96%.

In addition, dose reductions from 5% to 98% were calculated for organs normally protected by the apron, very likely because the apron of the ZG system has a higher lead thickness than a conventional apron. One should keep in mind, however, that the absolute dose to those organs is usually low when a lead apron is used, and can be 100 times lower than the dose to the unprotected left eye lens for instance. These reductions lead to decrease in effective dose around 60% for the different projections.

Surprisingly, simulations also showed dose increases for some internal organs situated on the left side of the staff body in RLAT projections. For instance, 18% dose increase was observed at the lung and the stomach. Aside from the low magnitude of the dose to those organs covered by the lead apron as already mentioned, this was probably caused by an inaccurate modelling of the ZG, in particular the shoulder and upper arm protection: while this protection is flexible and in contact with the operator arms (Figure 5), this is not the case for the ZG system modelled in the simulations (Figure 14).

Measurements at the level of the upper arm in hospital I did show a clear reduction of the dose due to the elbow and arm protection. In hospital K, the exposure for the ring finger of both hands increased considerably as compared to those resulting in the procedures performed without ZG system but with the ceiling suspended lead shield instead. However, the operators were not experienced with ZG system which could result in different position or manipulations as compared to usual practice.

5. Future work

Various configurations were simulated using MC calculations and hundreds of clinical measurements were performed on the staff or on phantoms. However, the influence of some parameters would deserve to be further investigated.

MC simulations and phantom measurements investigated separately the efficiency of the RP devices. The combined efficiency of RP devices (e.g. drape and ceiling-suspended screen) was only investigated by means of clinical measurements on the staff. Complementary MC simulations could lead to a better understanding of these combined effects and explain discrepancy between simulations and clinical measurements.

Only one x-ray beam quality was presented for the simulations although sensitivity studies were performed for some devices in PA projection but were not presented here. These showed no significant influence on the device efficiency. However, the influence of higher energy beam qualities should be further investigated.

Simulations and measurements were performed for configurations and procedures commonly used in IC and considering three heads orientations where relevant. A large variability of the RP efficiency was observed. The influence of other interventional practice should also be investigated, in particular for different treatment regions, different access routes (position of the staff with respect to the primary x-ray beam) and different staff positions and anatomies. The use of a motion tracking system (Lombardo and Zankl 2018) to automatically generate a library of realistic staff position would be an invaluable tool for that purpose.

6. Recommendations

Formulating recommendations is a challenging task since the potential for dose reduction of most devices strongly depends on their design and the exposure conditions. For those personal devices that are directly aimed at protecting the head region, such as the lead glasses and the masks, an extended face coverage and the smallest possible gap between the face and the device are crucial parameters to ensure adequate protection. By contrast, some devices, such as the ceiling-suspended screen (not studied in the present study) and the Zero gravity suspended system, can offer significant dose reduction in most circumstances if they are properly used.

The user should also keep in mind that the dose reduction efficiency as measured on the staff or on phantoms, and as calculated in MC simulations can differ. In addition to the efficiency, the absolute dose should be considered when evaluating the performances of a RP device: low dose reduction efficiency for a specific tissue which is exposed to very low dose might not be of concern for radiation protection, while low dose reduction to a highly exposed tissue is of concern. For illustration purposes, the potential for brain dose reduction of three specific devices (a lead mask (M1), a lead cap and the ZG suspended system) over a 25-years career was calculated using efficiency from phantom measurements as presented in the report (Table 20). In particular, the following assumptions were made:(i) a physician who performed yearly 550 PCI procedures; (ii) an average P_{KA} of 3000 µGy.m² per PCI procedure; and (iii) respective P_{KA} contribution from PA, LAO, LLAT and RAO projections equals 30%, 30%, 10% and 30%. The difference in cumulative doses over the whole career are considerable, with dose savings from 15 mSv to 154 mSv. All protective tools lead to a significant decrease in brain dose over the career.

Table 20: Example of potential dose reduction over a 25-years career using specific a lead mask, a lead cap or the ZG suspended system for a physician who performed yearly 550 PCI procedures. Dose reduction factors from comparable configurations from phantom measurements are used; absolute brain dose values are taken from phantom measurements as presented in the report. An average PCI procedure is assumed to deliver 3000 µGy.m² and be composed of PA, LAO, LLAT and RAO projections with respective contributions of 30%, 30%, 10% and 30%.

	Phantom measurements			
	Ref. dose mGy (no protection)	**Mask M1 mGy**	**Lead cap mGy**	**ZG mGy**
PA (30%)	0.003	0.003	0.003	0.001
LAO 30/45 (30%)	0.005	0.004	0.004	0.000
LLAT (10%)	0.003	0.002	0.003	0.000
RAO 30/45 (30%)	0.002	0.002	0.002	0.000*
Dose per procedure [mGy]	0.013	0.011	0.012	0.002
Annual brain dose [mGy]	7.2	6.2	6.6	1.0
Annual dose reduction [mGy]	-	0.9	0.6	6.2
Career cumulative dose [mGy]	**179**	**156**	**164**	**24.8**

*Reduction efficiency from LAO 30 used

Besides, not all combinations of factors that can adversely affect the efficiency of the RP devices were investigated. Although various configurations were simulated using MC calculations and hundreds of

clinical measurements were performed, only a limited number of RP device models and designs can be tested. In particular, clinical practice in other hospitals can strongly differ from the ones observed during the measurement campaigns, not forgetting the potential effect arising from difference in physician anatomy and posture. The lead equivalence of the RP device should not be overlooked either, since it might be considerably lower than the one stated on the device label. Therefore, reported efficiency levels of a RP device, whether reported in the scientific literature or claimed by the manufacturers, should always be considered with caution and, if feasible, validated in the planned conditions of use.

Finally, in addition to the mere dose reduction efficiency, factors not directly related to radiation protection such as ergonomics, frequency of use, expected exposure, price and protection of other organs, should also be considered in the selection process.

Specific advantages and disadvantages of each of the five RP devices tested are report below. Although this list is based on procedures and configurations frequently used in IC practice, the results should apply to other specialities provided the configurations are similar.

Caps

- **PRO: potential for dose decrease to the brain in specific conditions**

  (MC) Results of MC simulations showed a dose reduction of 35% averaged over several configurations. (PH) Phantom measurements showed a considerably lower average reduction (7%), indicating the great influence of the irradiation conditions.

- **PRO: protection comparable for lead and lead-free caps**

  (MC) Results of MC simulations showed comparable reduction of the brain dose, ranging from 10% to 43% depending on the configuration.

- **PRO: more comfortable than the lead mask**

  In general, a lead cap is considerably lighter than a mask (e.g. 3 times lower weight for a lead cap) and does not impair vision.

- **CON: strongly depends on staff position and head orientation**

  (MC) The closer the staff to the centre of the incident x-ray field, the smaller the dose reduction. Indeed, if the staff is close to the beam, the backscattered x-rays reach the brain through region not covered by the cap. The height of the staff (and of the table) has logically an influence too.

- **CON: dose reduction to the brain is not the attenuation characteristics of the device**

  The lead equivalence of the cap and the resulting x-ray attenuation in a direct x-ray beam stated by the manufacturer are not representative of the dose reduction to the brain. (MC and PH). Therefore, dosimeters placed under the cap may strongly overestimate the dose reduction to the brain.

- **CON: only limited parts of the brain are protected**

  (MC & PH) MC simulations and phantom measurements have shown that only some upper parts of the brain were protected. Dose reduction was lower for all regions when the physician was close to the primary beam; further away from the beam, protection of the hippocampus and the right side of the white matter was low.

Masks

- **PRO: potential for dose decrease to eyes and brain**

  (MC) MC simulations indicated average dose reduction of 65% and 25% to the eyes and the brain, respectively. (PH) Phantom measurements indicated dose reduction to the eye and the brain up to 10% and 17%, respectively. The mask was the most effective to protect the brain for LLAT projection which delivers the highest exposure to the physician.

- **PRO: More efficient than a lead cap for protecting the brain**

  (MC & PH) Both simulations and measurements showed that a mask was more efficient than a cap to protect the brain.

- **PRO / CON: efficiency strongly affected by design**

  (MC) From three mask models investigated, the length of the mask and the lateral protections had a strong effect on the efficiency. Different designs could result in an additional 50% reduction in specific configurations. Long and enveloping masks offer a better protection.

- **PRO / CON: efficiency strongly affected by staff position and head orientation**

  (MC) The staff distance from the x-ray beam entrance on the patient and the orientation of the staff head with respect to the beam could have a strong influence on the mask efficiency. For instance, the dose reduction to the brain and the left eye were very limited close to the beam (on average, 12.5 % and 0.5 %, respectively), further away from the beam, the reduction improved (on average, 43% and 4.1 %, respectively). *(PH) The mask may not be effective in the frequently used PA projection in case, it cannot be adjusted close enough to the physician's face.*

- **CON: heavier than lead-free cap**

  A mask can weigh about 400 g, while a lead-free cap can be three to four times lighter.

- **CON: dose decrease to eye-lens dosimeter is not representative of eye lens dose decrease**

  (MC& PH) Dedicated eye-lens dosimeter underestimates the actual dose to the eye lens.

- **CON: some parts of the brain are less protected than others**

  (MC& PH) Results from both simulations and measurements showed that the protection might be very heterogeneous and only limited regions, closer to the skull, might be protected. For instance, (MC) dose reduction for the left side of the white matter could twice as much as for the right side. However, when no shielding was used, the right side was exposed to lower absolute doses than the left side.

Drapes

- **PRO: significant dose decrease to hands, fingers and whole body dosimeter**

  (ST) Clinical measurements showed considerable dose reduction to the hand and fingers (20-40%) and to WB dosimeter (30-50%). (MC) Although MC simulations supported the decrease to the hands, no effect was observed on the WB dosimeter.

- **PRO: no significant effect on patient dose**

  Literature) MC simulations and phantom measurements have shown no significant effect on patient dose if the drape stays outside the primary beam.

- **PRO / CON: influence of the positioning**

  (MC and PH) The drape efficiency increases when it is placed closer to the primary beam and when it covers the patient side closer to the cardiologist without gap at the level of the table. In addition, the drape protects better the organs in its direct vicinity such as the hands and the forearms.

- **CON: limited effect on eyes and brain**

  (ST) Measurements on staff have showed dose reduction up to 50% to eye lens; however, this was not observed in all participating hospitals, possibly indicating a strong influence of local practice. (MC) Besides, MC simulations showed very limited dose reduction to eye lens and brain, between 0 to 10%.

- **CON: risk to increase the dose if in the beam**

  (Literature) If the drape is positioned partially in the primary beam, it will interfere with the automatic exposure system, which will increase the delivered dose.

Aprons

- **PRO: protection comparable to that of conventional lead aprons for covered organs**

  (MC) For two models of lead-free and one model of lead apron, results of MC simulations showed comparable reduction of the effective dose E, ranging from 71% to 94%. (ST) From routine dosimetry measurements, no significant dose increase was observed for staff who changed a conventional lead apron for a light lead or a lead-free apron.

- **PRO: potentially lower weight than conventional aprons**

  (Literature) Lead apron have been known to be the cause of back-pain. Lead-free apron can be lighter, although the weight difference might be little.

- **CON: Lead-equivalence claimed by manufacturers might not be met**

  (Literature) Studies reported many cases of lead equivalence thicknesses being smaller than the values claimed by the manufacturers.

- **CON: Dose enhancement for superficial organs with lead-free aprons**

  (Literature) Dose enhancement reported in the literature for superficial organs (breast for instance) with lead-free apron has to be further investigated in realistic clinical conditions as a possibly increased risk for cancer induction cannot be fully excluded.

Zero-Gravity suspended system

- **PRO: protection comparable to that of conventional lead aprons for covered organs**

  (PH& ST) For the regions normally covered by the lead apron, including the WB dosimeter, no meaningful difference could be observed during measurements. (MC) Simulations have shown a potential for dose reduction to organ normally covered by the lead apron.

- **PRO: significant dose decrease to the eyes and brain**

  (ST) In clinical practice, 75% and 90% reduction to the eyes and the whole body dose were observed, respectively, when compared to ceiling suspended shield only. (MC) MC simulations delivered comparable reduction magnitude when comparing the device to a configuration with only a lead apron.

- **PRO: lower weight on the operator than lead apron**

  (ST) Thanks to the suspending system, none of the weight of the ZG lies on the operator.

- **CON: limited visibility of pedals**

  (ST) Due to the design of the ZG and its face mask, the operator cannot see the pedals of the X-ray system.

- **CON: big investment**

  Compared to the price of conventional protective equipment, the price of the ZG is considerably higher and might not be accessible to all medical centres.

7. Conclusions

The efficiency of five RP devices to reduce staff dose were assessed using MC simulations and measurements on the staff and phantoms. (i) lead and lead-free caps and masks have a potential for brain and eye lens (for the latter); (ii) Lead and lead-free- drapes positioned on the patients have a clear effect on the exposure of the staff fingers and potentially on the whole-body and the eye lens dose; (iii) lead-free- aprons can offer comparable protection to a lead apron; (iv) and the ZG system offers a considerable dose reduction to all organs covered. Nevertheless, it should not be overlooked that even if similar trends were generally found between measurements and simulations, discrepancies were frequent because numerous factors such as device design and local clinical practice can strongly affect the shielding efficiency.

8. References

Alazzoni A, Gordon C L, Syed J, Natarajan M K, Rokoss M, Schwalm J D, Mehta S R, Sheth T, Valettas N, Velianou J, Pandie S, Al Khdair D, Tsang M, Meeks B, Colbran K, Waller E, Fu Lee S, Marsden T and Jolly S S 2015 Randomized Controlled Trial of Radiation Protection With a Patient Lead Shield and a Novel, Nonlead Surgical Cap for Operators Performing Coronary Angiography or Intervention *Circ Cardiovasc Interv***8** e002384

Alderson, S W, Lanzl, L H Rollins and M Spira, J1962 An instrumented phantom system for analog computation of treatment plans 185-195.

Andreassi M G, Piccaluga E, Gargani L, Sabatino L, Borghini A, Faita F, Bruno R M, Padovani R, Guagliumi G and Picano E 2015 Subclinical carotid atherosclerosis and early vascular aging from long-term low-dose ionizing radiation exposure: a genetic, telomere, and vascular ultrasound study in cardiac catheterization laboratory staff *JACC Cardiovasc Interv***8** 616-27

Andreassi M G, Piccaluga E, Guagliumi G, Del Greco M, Gaita F and Picano E 2016 Occupational Health Risks in Cardiac Catheterization Laboratory Workers *Circ Cardiovasc Interv***9** e003273

Aral N, Duch M A and Ardanuy M 2020 Material characterization and Monte Carlo simulation of lead and non-lead X-Ray shielding materials *Radiation Physics and Chemistry***174**

Behrens R, Dietze G and Zankl M 2009 Dose conversion coefficients for electron exposure of the human eye lens *Phys Med Biol***54** 4069-87

Ciraj-Bjelac O, Rehani M M, Sim K H, Liew H B, Vano E and Kleiman N J 2010 Risk for radiation-induced cataract for staff in interventional cardiology: is there reason for concern? *Catheter Cardiovasc Interv***76** 826-34

Domienik-Andrzejewska J, Ciraj-Bjelac O, Askounis P, Covens P, Dragusin O, Jacob S, Farah J, Gianicolo E, Padovani R, Teles P, Widmark A and Struelens L 2018 Past and present work practices of European interventional cardiologists in the context of radiation protection of the eye lens-results of the EURALOC study *J Radiol Prot***38** 934-50

Fetterly K A, Magnuson D J, Tannahill G M, Hindal M D and Mathew V 2011 Effective use of radiation shields to minimize operator dose during invasive cardiology procedures *JACC Cardiovasc Interv***4** 1133-1139

Fetterly K, Schueler B, Grams M, Sturchio G, Bell M and Gulati R 2017 Head and Neck Radiation Dose and Radiation Safety for Interventional Physicians *JACC Cardiovasc Interv***10** 520-528

Grabowicz W, Domienik-Andrzejewska J, Masiarek K, Gornik T, Grycewicz T, Brodecki M and Lubinski A 2017 Effectiveness of pelvic lead blanket to reduce the doses to eye lens and hands of interventional cardiologists and assistant nurses *J Radiol Prot***37** 715-27

Haussen D C, Van Der Bom I M J and Nogueira R G 2016 A prospective case control comparison of the ZeroGravity system versus a standard lead apron as radiation protection strategy in neuroendovascular procedures *Journal of NeuroInterventional Surgery* **8** 1052

Honorio da Silva E, Martin C J, Vanhavere F and Buls N 2020 A study of the underestimation of eye lens dose with current eye dosimeters for interventional clinicians wearing lead glasses *J Radiol Prot* **40** 215-24

ICRP 2007 ICRP publication 103: The 2007 Recommendations of the International Commission on Radiological Protection*Annals of the ICRP* **37**

ICRP 2009 ICRP publication 110: Adult Reference Computational Phantoms *Annals of the ICRP* **39** 1-166

International Organization for Standardization 2004 X and gamma reference radiation for calibrating dosemeters and doserate meters and for determining their responseas a function of photon energy—Part 4: Calibration ofarea and personal dosemeters in low energy X reference radiation fields. ISO 4037-4.

Karadag B, Ikitimur B, Durmaz E, Avci B K, Cakmak H A, Cosansu K and Ongen Z 2013 Effectiveness of a lead cap in radiation protection of the head in the cardiac catheterisation laboratory *EuroIntervention* **9** 754-6

Koukorava C, Carinou E, Ferrari P, Krim S and Struelens L 2011 Study of the parameters affecting operator doses in interventional radiology using Monte Carlo simulationsRadiation Measurements **46** (11) 1216-1222

Koukorava C, Farah J, Struelens L, Clairand I, Donadille L, Vanhavere F and Dimitriou P 2014 Efficiency of radiation protection equipment in interventional radiology: a systematic Monte Carlo study of eye lens and whole body doses. Journal of Radiological Protection **34**

Lombardo P and Zankl M 2018 D9.104: Database of phantom of different statures and postures.

Marshall et al., 1992, An investigation into the effect of protective devices on the dose to radiosensitive organs in the head and neck, Br J Radiol; 65(777):799-802. doi: 10.1259/0007-1285-65-777-799. PMID: 1393418.

McCutcheon K, Vanhaverbeke M, Pauwels R, Dabin J, Schoonjans W, Bennett J, Adriaenssens T, Dubois C, Sinnaeve P and Desmet W 2020 Efficacy of MAVIG X-Ray Protective Drapes in Reducing Operator Radiation Dose in the Cardiac Catheterization Laboratory: A Randomized Controlled Trial *Circ Cardiovasc Interv* CIRCINTERVENTIONS120009627

Roguin A, Goldstein J and Bar O 2012 Brain tumours among interventional cardiologists: a cause for alarm? Report of four new cases from two cities and a review of the literature *Eurointervention***7** 1081-6

Roguin A, Goldstein J, Bar O and Goldstein J A 2013 Brain and neck tumors among physicians performing interventional procedures *Am J Cardiol***111** 1368-72

Saldarriaga Vargas C, Struelens L and Vanhavere F 2018 The Challenges in the Estimation of the Effective Dose When Wearing Radioprotective Garments *Radiat Prot Dosimetry***178** 101-11

Sans Merce M, Korchi A M, Kobzeva L, Damet J, Erceg G, Marcos Gonzalez A, Lovblad K O and Mendes Pereira V 2016 The value of protective head cap and glasses in neurointerventional radiology *J Neurointerv Surg***8** 736-40

Savage C, Seale Iv T M, Shaw C J, Angela B P, Marichal D and Rees C R 2013 Evaluation of a Suspended Personal Radiation Protection System vs. Conventional Apron and Shields in Clinical Interventional Procedures *Open Journal of Radiology***03** 143-51

Schlattl H, Zankl M, Eder H and Hoeschen C 2007 Shielding properties of lead-free protective clothing and their impact on radiation doses *Med Phys***34** 4270-80

Silva E, Vanhavere F, Struelens L, Covens P and Buls N 2017 Effect of protective devices in the radiation dose received by the brain of interventional cardiologists *Eurointervention*

Uthoff H, Pena C, West J, Contreras F, Benenati J F, Katzen, B T 2013 Evaluation of novel disposable, light-weight radiation protection devices in an interventional radiology setting: a randomized controlled trial *AJR Am JRoentgenol***200** 915-920.

Vano E, Kleiman N J, Duran A, Romano-Miller M and Rehani M M 2013 Radiation-associated Lens Opacities in Catheterization Personnel: Results of a Survey and Direct Assessments *Journal of Vascular and Interventional Radiology***24** 197-204

Zubal I G, Harrell C R, Smith E O, Rattner Z, Gindi G and Hoffer P B 1994 COMPUTERIZED 3-DIMENSIONAL SEGMENTED HUMAN ANATOMY *Medical Physics***21** 299-302

9. Annex: Literature review: reference list

Apron

Finnerty, M., and P. C. Brennan. 2005 Protective Aprons in Imaging Departments: Manufacturer Stated Lead Equivalence Values Require Validation. [In English]. European Radiology 15, no. 7 (2005/07/01 2005): 1477-84.

Jones, A. K., and L. K. Wagner. 2013 On the (F)Utility of Measuring the Lead Equivalence of Protective Garments. [In eng]. Med Phys 40, no. 6 (Jun 2013): 063902.

Peters, S. M. B., D. Zweers, F. de Lange, and J. E. M. Mourik. 2017 Lead Composite Vs. Nonlead Protective Garments: Which Are Better? A Multivendor Comparison. RadiatProt Dosimetry 175, no. 4 (Aug 01 2017): 460-65.

Zuguchi, M., K. Chida, M. Taura, Y. Inaba, A. Ebata, and S. Yamada. 2008 Usefulness of Non-Lead Aprons in Radiation Protection for Physicians Performing Interventional Procedures. RadiatProt Dosimetry 131, no. 4 (2008): 531-4.

Cabin

Dragusin, O., Weerasooriya, R., Jais, P., Hocini, M., Ector, J., Takahashi, Y., Haissaguerre, M., Bosmans, H. and Heidbuchel, H. (2007). "Evaluation of a radiation protection cabin for invasive electrophysiological procedures." Eur Heart J 28(2): 183-189.

Maleux, G., Bergans, N., Bosmans, H. and Bogaerts, R. (2016). "Radiation Protection Cabin for Catheter-Directed Liver Interventions: Operator Dose Assessment." RadiatProt Dosimetry 170(1-4): 274-278.

Ploux, S., Ritter, P., Haissaguerre, M., Clementy, J. and Bordachar, P. (2010). "Performance of a radiation protection cabin during implantation of pacemakers or cardioverter defibrillators." J CardiovascElectrophysiol 21(4): 428-430.

Ploux, S., Jesel, L., Eschalier, R., Amraoui, S., Ritter, P., Haissaguerre, M. and Bordachar, P.(2014). "Performance of a radiation protection cabin during extraction of cardiac devices." Can J Cardiol 30(12): 1602-1606.

Cap

Alazzoni, A., C. L. Gordon, J. Syed, M. K. Natarajan, M. Rokoss, J. D. Schwalm, S. R. Mehta, et al. 2015 Randomized Controlled Trial of Radiation Protection with a Patient Lead Shield and a Novel, Nonlead Surgical Cap for Operators Performing Coronary Angiography or Intervention. CircCardiovascInterv 8, no. 8 (Aug 2015): e002384.

Fetterly, K., B. Schueler, M. Grams, G. Sturchio, M. Bell, and R. Gulati. 2017b Head and Neck Radiation Dose and Radiation Safety for Interventional Physicians. JACC CardiovascInterv 10, no. 5 (Mar 13 2017): 520-28.

Karadag, B., B. Ikitimur, E. Durmaz, B. K. Avci, H. A. Cakmak, K. Cosansu, and Z. Ongen. 2013 Effectiveness of a Lead Cap in Radiation Protection of the Head in the Cardiac Catheterisation Laboratory. EuroIntervention 9, no. 6 (Oct 2013): 754-6.

Kuon, E., J. Birkel, M. Schmitt, and J.B. Dahm. 2003 Radiation Exposure Benefit of a Lead Cap in Invasive Cardiology. Interventional cardiology and surgery 89 (2003): 1205-10.

Lemesre, C., D. Graf, L. Bisch, P. Carroz, N. Cherbuin, J. Damet, L. Desorgher, C. H. Siklody, M. Le Bloa, Mathieu, P. Pascale and E. Pruvot. 2020 Efficiency of the RADPAD Surgical Cap in Reducing Brain Exposure During Pacemaker and Defibrillator Implantation. JACC: Clinical Electrophysiology.

Reeves, R. R., L. Ang, J. Bahadorani, J. Naghi, A. Dominguez, V. Palakodeti, S. Tsimikas, M. P. Patel, and E. Mahmud. 2015 Invasive Cardiologists Are Exposed to Greater Left Sided Cranial Radiation: The Brain Study (Brain Radiation Exposure and Attenuation During Invasive Cardiology Procedures). JACC CardiovascInterv 8, no. 9 (Aug 17 2015): 1197-206.

Sans Merce, M., A. M. Korchi, L. Kobzeva, J. Damet, G. Erceg, A. Marcos Gonzalez, K. O. Lovblad, and V. Mendes Pereira. 2016 The Value of Protective Head Cap and Glasses in Neurointerventional Radiology. J NeurointervSurg 8, no. 7 (Jul 2016): 736-40.

Silva, E., F. Vanhavere, L. Struelens, P. Covens, and N. Buls. 2017 Effect of Protective Devices in the Radiation Dose Received by the Brain of Interventional Cardiologists. Eurointervention (2017).

Uthoff, H., C. Pena, J. West, F. Contreras, J. F. Benenati, and B. T. Katzen. 2013 Evaluation of Novel Disposable, Light-Weight Radiation Protection Devices in an Interventional Radiology Setting: A Randomized Controlled Trial. AJR Am J Roentgenol 200, no. 4 (Apr 2013): 915-20.

Ceiling-suspended screen

Batlivala, S. P., D. Magill, M. A. Felice, V. Jones, Y. Dori, M. J. Gillespie, J. J. Rome, and A. C. Glatz. 2015 The Effect of Radiation Shields on Operator Exposure During Congenital Cardiac Catheterisation. RadiationProtectionDosimetry (2015).

Domienik, J., Bissinger, A., W. Grabowicz, Ł. Jankowski, R. Kręcki, M. Makowski, K. Masiarek, M. Plewka, A. Lubiński and J.Z. Peruga. 2016. "The impact of various protective tools on the dose reduction in the eye lens in an interventional cardiology—clinical study." Journal of Radiological Protection 36(2): 309-318.

Fetterly, K. A., D. J. Magnuson, G. M. Tannahill, M. D. Hindal, and V. Mathew. 2011 Effective Use of Radiation Shields to Minimize Operator Dose During Invasive Cardiology Procedures. JACC CardiovascInterv 4, no. 10 (Oct 2011): 1133-9.

Galster, M., C. Guhl, M. Uder, and R. Adamus. 2013 [Exposition of the Operator's Eye Lens and Efficacy of Radiation Shielding in Fluoroscopically Guided Interventions]. Rofo 185, no. 5 (May 2013): 474-81.

Kim, K. P., and D. L. Miller. 2009 Minimising Radiation Exposure to Physicians Performing Fluoroscopically Guided Cardiac Catheterisation Procedures: A Review. RadiatProt Dosimetry 133, no. 4 (Feb 2009): 227-33.

Koukorava, C., E. Carinou, P. Ferrari, S. Krim, and L. Struelens. 2011 Study of the Parameters Affecting Operator Doses in Interventional Radiology Using Monte Carlo Simulations. Radiation Measurements 46, no. 11 (2011): 1216-22.

Leyton, Fernando, Maria S. Nogueira, Jamil Saad, Jorge A. dos Santos, Eliseo Vano, Marcio A. Oliveira, and Carlos Ubeda. 2014 Scatter Radiation Dose at the Height of the Operator's Eye in Interventional Cardiology. Radiation Measurements 71 (2014): 349-54.

Maeder, M., H. P. Brunner-La Rocca, T. Wolber, P. Ammann, H. Roelli, F. Rohner, and H. Rickli. 2006 Impact of a Lead Glass Screen on Scatter Radiation to Eyes and Hands in Interventional Cardiologists. [In eng]. Catheter CardiovascInterv 67, no. 1 (Jan 2006): 18-23.

Magee, J. S., C. J. Martin, V. Sandblom, M. J. Carter, A. Almen, A. Cederblad, P. Jonasson, and C. Lundh. 2014 Derivation and Application of Dose Reduction Factors for Protective Eyewear Worn in Interventional Radiology and Cardiology. J RadiolProt 34, no. 4 (Dec 2014): 811-23.

Martin, C. J., J. S. Magee, V. Sandblom, A. Almen, and C. Lundh. 2015 Eye Dosimetry and Protective Eyewear for Interventional Clinicians. RadiatProt Dosimetry 165, no. 1-4 (Jul 2015): 284-8.

Principi, S., M. Ginjaume, M. A. Duch, R. M. Sanchez, J. M. Fernandez, and E. Vano. 2015b Influence of Dosemeter Position for the Assessment of Eye Lens Dose During Interventional Cardiology. [In eng]. RadiatProt Dosimetry 164, no. 1-2 (Apr 2015): 79-83.

Silva, E., F. Vanhavere, L. Struelens, P. Covens, and N. Buls. 2017 Effect of Protective Devices in the Radiation Dose Received by the Brain of Interventional Cardiologists. Eurointervention (2017).

Thornton, R. H., L. T. Dauer, J. P. Altamirano, K. J. Alvarado, J. St Germain, and S. B. Solomon. 2010 Comparing Strategies for Operator Eye Protection in the Interventional Radiology Suite. J VascIntervRadiol 21, no. 11 (Nov 2010): 1703-7.

Drape

Alazzoni, A., C. L. Gordon, J. Syed, M. K. Natarajan, M. Rokoss, J. D. Schwalm, S. R. Mehta, et al. 2015 Randomized Controlled Trial of Radiation Protection with a Patient Lead Shield and a Novel, Nonlead Surgical Cap for Operators Performing Coronary Angiography or Intervention. CircCardiovascInterv 8, no. 8 (Aug 2015): e002384.

Batlivala, S. P., D. Magill, M. A. Felice, V. Jones, Y. Dori, M. J. Gillespie, J. J. Rome, and A. C. Glatz. 2015 The Effect of Radiation Shields on Operator Exposure During Congenital Cardiac Catheterisation. Radiation Protection Dosimetry (2015).

Brambilla, M., E. Occhetta, M. Ronconi, L. Plebani, A. Carriero, and P. Marino. 2010 Reducing Operator Radiation Exposure During Cardiac Resynchronization Therapy. Europace 12, no. 12 (Dec 2010): 1769-73.

Dromi, Sergio, Bradford J. Wood, Jay Oberoi, and ZivNeeman. 2006 Heavy Metal Pad Shielding During Fluoroscopic Interventions. Journal of vascular and interventional radiology : JVIR 17, no. 7 (2006): 1201-06.

Ertel, A., J. Nadelson, A. R. Shroff, R. Sweis, D. Ferrera, and M. I. Vidovich. 2012 Radiation Dose Reduction During Radial Cardiac Catheterization: Evaluation of a Dedicated Radial Angiography Absorption Shielding Drape. ISRN Cardiol 2012 (2012): 769167.

Fetterly, K. A., D. J. Magnuson, G. M. Tannahill, M. D. Hindal, and V. Mathew. 2011 Effective Use of Radiation Shields to Minimize Operator Dose During Invasive Cardiology Procedures. JACC CardiovascInterv 4, no. 10 (Oct 2011): 1133-9.

Germano, J. J., G. Day, Gregorious D., Natarajan V., and Cohen T. 2005 A Novel Radiation Protection Drape Reduces Radiation Exposure During Fluoroscopy Guided Electrophysiology Procedures. . J Invasive Cardiol. 17, no. 9 (2005): 469-72.

Gilligan, Paddy, J. Lynch, H. Eder, S. Maguire, E. Fox, B. Doyle, I. Casserly, H. McCann, and D. Foley. 2015 Assessment of Clinical Occupational Dose Reduction Effect of a New Interventional Cardiology Shield for Radial Access Combined with a Scatter Reducing Drape. Catheterization and Cardiovascular Interventions 86, no. 5 (2015): 935-40.

Grabowicz W, Domienik-Andrzejewska J, Masiarek K, Gornik T, Grycewicz T, Brodecki M and Lubinski A 2017 Effectiveness of pelvic lead blanket to reduce the doses to eye lens and hands of interventional cardiologists and assistant nurses J RadiolProt 37 715-27

Iqtidar A F, Jeon C, Rothman R, Snead R and Pyne C T 2013 Reduction in operator radiation exposure during transradial catheterization and intervention using a simple lead drape American heart journal 165 293-8

Irani, Z., B. Alexander, D. Zhang, B. Liu, B. Ghoshhajra, and R. Oklu. 2014 Novel Lead-Free Drape Applied to the X-Ray Detector Protects against Scatter Radiation in the Angiography Suite. [In eng]. J Vasc Interv Radiol 25, no. 8 (Aug 2014): 1200-8.

Jones, M. A., M. Cocker, R. Khiani, P. Foley, N. Qureshi, K. C. Wong, K. Rajappan, and T. R. Betts. 2014 The Benefits of Using a Bismuth-Containing, Radiation-Absorbing Drape in Cardiac Resynchronization Implant Procedures. [In eng]. Pacing Clin Electrophysiol 37, no. 7 (Jul 2014): 828-33.

King, Jerry N., Anna M. Champlin, Charles A. Kelsey, and David A. Tripp. 2002 Using a Sterile Disposable Protective Surgical Drape for Reduction of Radiation Exposure to Interventionalists. American Journal of Roentgenology 178, no. 1 (2002/01/01 2002): 153-57.

Kloeze, C., E. G. Klompenhouwer, P. J. Brands, M. R. van Sambeek, P. W. Cuypers, and J. A. Teijink. 2014 Use of Disposable Radiation-Absorbing Surgical Drapes Results in Significant Dose Reduction During Evar Procedures. Eur J Vasc Endovasc Surg 47, no. 3 (Mar 2014): 268-72.

Lange, H. W., and H. von Boetticher. 2012 Reduction of Operator Radiation Dose by a Pelvic Lead Shield During Cardiac Catheterization by Radial Access: Comparison with Femoral Access. JACC Cardiovasc Interv 5, no. 4 (Apr 2012): 445-9.

Martin, C. J., J. S. Magee, V. Sandblom, A. Almen, and C. Lundh. 2015 Eye Dosimetry and Protective Eyewear for Interventional Clinicians. Radiat Prot Dosimetry 165, no. 1-4 (Jul 2015): 284-8.

McCutcheon K, Vanhaverbeke M, Pauwels R, Dabin J, Schoonjans W, Bennett J, Adriaenssens T, Dubois C, Sinnaeve P and Desmet W 2020 Efficacy of MAVIG X-Ray Protective Drapes in Reducing Operator Radiation Dose in the Cardiac Catheterization Laboratory: A Randomized Controlled Trial Circ Cardiovasc Interv CIRCINTERVENTIONS120009627

Muniraj, Thiruvengadam, Harry R. Aslanian, Loren Laine, James Farrell, Maria M. Ciarleglio, Yanhong Deng, Henry Ho, and Priya A. Jamidar. 2015 A Double-Blind, Randomized, Sham-Controlled Trial of the Effect of a Radiation-Attenuating Drape on Radiation Exposure to Endoscopy Staff During Ercp. Am J Gastroenterol 110, no. 5 (05//print 2015): 690-96.

Murphy, John C., Karen Darragh, Simon J. Walsh, and Colm G. Hanratty. 2011 Efficacy of the Radpad Protective Drape During Real World Complex Percutaneous Coronary Intervention Procedures. The American Journal of Cardiology 108, no. 10 (11/15/ 2011): 1408-10.

Musallam, A., I. Volis, S. Dadaev, E. Abergel, A. Soni, S. Yalonetsky, A. Kerner, and A. Roguin. 2015 A Randomized Study Comparing the Use of a Pelvic Lead Shield During Trans-Radial Interventions: Threefold Decrease in Radiation to the Operator but Double Exposure to the Patient. Catheterization and Cardiovascular Interventions 85, no. 7 (Jun 2015): 1164-70.

Ordiales, J. M., J. M. Nogales, R. Sanchez-Casanueva, E. Vano, J. M. Fernandez, F. J. Alvarez, J. Ramos, G. Martinez, and J. R. Lopez-Minguez. 2015 Reduction of Occupational Radiation Dose in Staff at the Cardiac Catheterisation Laboratory by Protective Material Placed on the Patient. RadiatProt Dosimetry 165, no. 1-4 (Jul 2015): 272-5.

Politi, L., G. Biondi-Zoccai, L. Nocetti, T. Costi, D. Monopoli, R. Rossi, F. Sgura, M. G. Modena, and G. M. Sangiorgi. 2012 Reduction of Scatter Radiation During Transradial Percutaneous Coronary Angiography: A Randomized Trial Using a Lead-Free Radiation Shield. [In eng]. Catheter CardiovascInterv 79, no. 1 (Jan 1 2012): 97-102.

Schneider, J. E., R. Sachar, W. W. Orrison, and P. W. Patton. 2010 Peripherial Vascular Intervention (Poster Abstracts Tct-399 to Tct-418). Journal of the American College of Cardiology 56, no. 13 Supplement (2010): B93.

Shorrock, D., G. Christopoulos, J. Wosik, A. Kotsia, B. Rangan, S. Abdullah, D. Cipher, S. Banerjee, and E. S. Brilakis. 2015 Impact of a Disposable Sterile Radiation Shield on Operator Radiation Exposure During Percutaneous Coronary Intervention of Chronic Total Occlusions. [In eng]. J Invasive Cardiol 27, no. 7 (Jul 2015): 313-6.

Simons, G. R., and W. W. Orrison, Jr. 2004 Use of a Sterile, Disposable, Radiation-Absorbing Shield Reduces Occupational Exposure to Scatter Radiation During Pectoral Device Implantation. [In eng]. Pacing Clin Electrophysiol 27, no. 6 Pt 1 (Jun 2004): 726-9.

Thornton, R. H., L. T. Dauer, J. P. Altamirano, K. J. Alvarado, J. St Germain, and S. B. Solomon. 2010 Comparing Strategies for Operator Eye Protection in the Interventional Radiology Suite. J Vasc Interv Radiol 21, no. 11 (Nov 2010): 1703-7.

Glasses

Burns, S., R. Thornton, L. T. Dauer, B. Quinn, D. Miodownik, and D. J. Hak. 2013 Leaded Eyeglasses Substantially Reduce Radiation Exposure of the Surgeon's Eyes During Acquisition of Typical Fluoroscopic Views of the Hip and Pelvis. J Bone Joint Surg Am 95, no. 14 (Jul 17 2013): 1307-11.

Domienik, J. and M. Brodecki 2016. The effectiveness of lead glasses in reducing the doses to eye lenses during cardiac implantation procedures performed using x-ray tubes above the patient table. J RadiolProt 36(2): N19-25.

Fetterly, K., B. Schueler, M. Grams, G. Sturchio, M. Bell, and R. Gulati. 2017b Head and Neck Radiation Dose and Radiation Safety for Interventional Physicians. JACC Cardiovasc Interv 10, no. 5 (Mar 13 2017): 520-28.

Galster, M., C. Guhl, M. Uder, and R. Adamus. 2013 [Exposition of the Operator's Eye Lens and Efficacy of Radiation Shielding in Fluoroscopically Guided Interventions]. Rofo 185, no. 5 (May 2013): 474-81.

Kirkwood, M. L., Klein, A., Guild, J., Arbique, G., Xi, Y., Tsai, S., Ramanan, B. and Timaran, C.. (2020). "Novel modification to leaded eyewear results in significant operator eye radiation dose reduction." J Vasc Surg.

Kim, K. P., and D. L. Miller. 2009 Minimising Radiation Exposure to Physicians Performing Fluoroscopically Guided Cardiac Catheterisation Procedures: A Review. Radiat Prot Dosimetry 133, no. 4 (Feb 2009): 227-33.

Koukorava, C., E. Carinou, P. Ferrari, S. Krim, and L. Struelens. 2011 Study of the Parameters Affecting Operator Doses in Interventional Radiology Using Monte Carlo Simulations. Radiation Measurements 46, no. 11 (2011): 1216-22.

Koukorava, C., J. Farah, L. Struelens, I. Clairand, L. Donadille, F. Vanhavere, and P. Dimitriou. 2014 Efficiency of Radiation Protection Equipment in Interventional Radiology: A Systematic Monte Carlo Study of Eye Lens and Whole Body Doses. Journal of Radiological Protection 34 (2014).

Magee, J. S., C. J. Martin, V. Sandblom, M. J. Carter, A. Almen, A. Cederblad, P. Jonasson, and C. Lundh. 2014 Derivation and Application of Dose Reduction Factors for Protective Eyewear Worn in Interventional Radiology and Cardiology. J RadiolProt 34, no. 4 (Dec 2014): 811-23.

Marshall, N. W., K. Faulkner, and H. Warren. 1992 Measured Scattered X-Ray Energy Spectra for Simulated Irradiation Geometries in Diagnostic Radiology. Med Phys 23, no. 7 (Jul 1996): 1271-6.

Martin, C. J. 2016 Eye Lens Dosimetry for Fluoroscopically Guided Clinical Procedures: Practical Approaches to Protection and Dose Monitoring. RadiatProt Dosimetry 169, no. 1-4 (Jun 2016): 286-91.

Martin, C. J., J. S. Magee, V. Sandblom, A. Almen, and C. Lundh. 2015 Eye Dosimetry and Protective Eyewear for Interventional Clinicians. RadiatProt Dosimetry 165, no. 1-4 (Jul 2015): 284-8.

McVey, S., A. Sandison, and D. G. Sutton. 2013 An Assessment of Lead Eyewear in Interventional Radiology. J RadiolProt 33, no. 3 (Sep 2013): 647-59.

Moore, W. E., G. Ferguson, and C. Rohrmann. 1980 Physical Factors Determining the Utility of Radiation Safety Glasses. MedicalPhysics (1980).

Domienik, J., Bissinger, A., W. Grabowicz, Ł. Jankowski, R. Kręcki, M. Makowski, K. Masiarek, M. Plewka, A. Lubiński and J.Z. Peruga. 2016. "The impact of various protective tools on the dose reduction in the eye lens in an interventional cardiology—clinical study." Journal of Radiological Protection 36(2): 309-318.

Doria, S., L. Fedeli, L, L. Redapi, S. Piffer, F. Rossi, A. Falivene, S. Busoni, G. Belli, C. Gori and A. Taddeucci2020 Addressing the efficiency of X-ray protective eyewear: Proposal for the introduction of a new comprehensive parameter, the Eye Protection Effectiveness (EPE). PhysicaMedica 70: 216-223.

Principi, S., C. Delgado Soler, M. Ginjaume, M. Beltran Vilagrasa, J. J. RoviraEscutia, and M. A. Duch. 2015a Eye Lens Dose in Interventional Cardiology. RadiatProt Dosimetry 165, no. 1-4 (Jul 2015): 289-93.

Principi, S., M. Ginjaume, M. A. Duch, R. M. Sanchez, J. M. Fernandez, and E. Vano. 2015b Influence of Dosemeter Position for the Assessment of Eye Lens Dose During Interventional Cardiology. [In eng]. RadiatProt Dosimetry 164, no. 1-2 (Apr 2015): 79-83.

Rivett, C., M. Dixon, L. Matthews, and N. Rowles. 2016 An Assessment of the Dose Reduction of Commercially Available Lead Protective Glasses for Interventional Radiology Staff. RadiatProt Dosimetry 172, no. 4 (Dec 2016): 443-52.

Sans Merce, M., A. M. Korchi, L. Kobzeva, J. Damet, G. Erceg, A. Marcos Gonzalez, K. O. Lovblad, and V. Mendes Pereira. 2016 The Value of Protective Head Cap and Glasses in Neurointerventional Radiology. J NeurointervSurg 8, no. 7 (Jul 2016): 736-40.

Silva, E., F. Vanhavere, L. Struelens, P. Covens, and N. Buls. 2017 Effect of Protective Devices in the Radiation Dose Received by the Brain of Interventional Cardiologists. Eurointervention (2017).

Strocchi, S., A. Chiaravalli, I. Veronese, and R. Novario. 2016 On-Field Evaluation of Operator Lens Protective Devices in Interventional Radiology. RadiatProt Dosimetry 171, no. 3 (Nov 2016): 382-88.

Sturchio G M, Newcomb R D, Molella R, Varkey P, Hagen P T and Schueler B A 2013 Protective Eyewear Selection for Interventional Fluoroscopy 2013 Health Phys. 104 S11-S6

Thornton, R. H., L. T. Dauer, J. P. Altamirano, K. J. Alvarado, J. St Germain, and S. B. Solomon. 2010 Comparing Strategies for Operator Eye Protection in the Interventional Radiology Suite. J Vasc Interv Radiol 21, no. 11 (Nov 2010): 1703-7.

van Rooijen, B. D., M. W. de Haan, M. Das, C. W. Arnoldussen, R. de Graaf, W. H. van Zwam, W. H. Backes, and C. R. Jeukens. 2014 Efficacy of Radiation Safety Glasses in Interventional Radiology. CardiovascInterventRadiol 37, no. 5 (Oct 2014): 1149-55.

Zett-Lobos, C. 2013 Protection against Ionizing Radiation by Leaded Glass Googles During Interventional Cardiology. Rev Med Chile 141 (2013).

Mask

Marshall, N. W., K. Faulkner, and H. Warren. 1992 Measured Scattered X-Ray Energy Spectra for Simulated Irradiation Geometries in Diagnostic Radiology. Med Phys 23, no. 7 (Jul 1996): 1271-6.

Other

Galster, M., C. Guhl, M. Uder, and R. Adamus. 2013 [Exposition of the Operator's Eye Lens and Efficacy of Radiation Shielding in Fluoroscopically Guided Interventions]. Rofo 185, no. 5 (May 2013): 474-81.

Gilligan, Paddy, J. Lynch, H. Eder, S. Maguire, E. Fox, B. Doyle, I. Casserly, H. McCann, and D. Foley. 2015 Assessment of Clinical Occupational Dose Reduction Effect of a New Interventional Cardiology Shield for Radial Access Combined with a Scatter Reducing Drape. Catheterization and Cardiovascular Interventions 86, no. 5 (2015): 935-40.

Mori, H., K. Koshida, O. Ishigamori, and K. Matsubara. 2014 A Novel Removable Shield Attached to C-Arm Units against Scattered X-Rays from a Patient's Side. [In English]. European Radiology 24, no. 8 (Aug 2014): 1794-99.

Table skirt

Batlivala, S. P., D. Magill, M. A. Felice, V. Jones, Y. Dori, M. J. Gillespie, J. J. Rome, and A. C. Glatz. 2015 The Effect of Radiation Shields on Operator Exposure During Congenital Cardiac Catheterisation. Radiation Protection Dosimetry (2015).

Galster, M., C. Guhl, M. Uder, and R. Adamus. 2013 [Exposition of the Operator's Eye Lens and Efficacy of Radiation Shielding in Fluoroscopically Guided Interventions]. Rofo 185, no. 5 (May 2013): 474-81.

Kim, K. P., and D. L. Miller. 2009 Minimising Radiation Exposure to Physicians Performing Fluoroscopically Guided Cardiac Catheterisation Procedures: A Review. RadiatProt Dosimetry 133, no. 4 (Feb 2009): 227-33.

Koukorava, C., E. Carinou, P. Ferrari, S. Krim, and L. Struelens. 2011 Study of the Parameters Affecting Operator Doses in Interventional Radiology Using Monte Carlo Simulations. Radiation Measurements 46, no. 11 (2011): 1216-22.

Theocharopoulos, N., J. Damilakis, K. Perisinakis, E. Manios, P. Vardas, and N. Gourtsoyiannis. 2006 Occupational Exposure in the Electrophysiology Laboratory: Quantifying and Minimizing Radiation Burden. Br J Radiol 79, no. 944 (Aug 2006): 644-51.

Thornton, R. H., L. T. Dauer, J. P. Altamirano, K. J. Alvarado, J. St Germain, and S. B. Solomon. 2010 Comparing Strategies for Operator Eye Protection in the Interventional Radiology Suite. J Vasc Interv Radiol 21, no. 11 (Nov 2010): 1703-7.

Table vertical extension

Batlivala, S. P., D. Magill, M. A. Felice, V. Jones, Y. Dori, M. J. Gillespie, J. J. Rome, and A. C. Glatz. 2015 The Effect of Radiation Shields on Operator Exposure During Congenital Cardiac Catheterisation. Radiation Protection Dosimetry (2015).

Behan, M., P. Haworth, P. Colley, M. Brittain, A. Hince, M. Clarke, A. Ghuran, M. Saha, and D. Hildick-Smith. 2010 Decreasing Operators' Radiation Exposure During Coronary Procedures: The Transradial Radiation Protection Board. [In eng]. Catheter Cardiovasc Interv 76, no. 1 (Jul 1 2010): 79-84.

Fetterly, K. A., D. J. Magnuson, G. M. Tannahill, M. D. Hindal, and V. Mathew. 2011 Effective Use of Radiation Shields to Minimize Operator Dose During Invasive Cardiology Procedures. JACC Cardiovasc Interv 4, no. 10 (Oct 2011): 1133-9.

Galster, M., C. Guhl, M. Uder, and R. Adamus. 2013 [Exposition of the Operator's Eye Lens and Efficacy of Radiation Shielding in Fluoroscopically Guided Interventions]. Rofo 185, no. 5 (May 2013): 474-81.

Thyroid collar

Marshall, N. W., K. Faulkner, and H. Warren. 1992 Measured Scattered X-Ray Energy Spectra for Simulated Irradiation Geometries in Diagnostic Radiology. Med Phys 23, no. 7 (Jul 1996): 1271-6.

Uthoff, H., C. Pena, J. West, F. Contreras, J. F. Benenati, and B. T. Katzen. 2013 Evaluation of Novel Disposable, Light-Weight Radiation Protection Devices in an Interventional Radiology Setting: A Randomized Controlled Trial. AJR Am J Roentgenol 200, no. 4 (Apr 2013): 915-20.

Zero Gravity suspended system

Fattal, P., and J. A. Goldstein. 2013 A Novel Complete Radiation Protection System Eliminates Physician Radiation Exposure and Leaded Aprons. [In English]. Catheterization and Cardiovascular Interventions 82, no. 1 (Jul 2013): 11-16.

Savage, Clare, Seale Iv, Thomas M., Shaw, Cathryn J., Angela, Bruner P., Marichal, Daniel and Rees, Chet R. 2013 Evaluation of a Suspended Personal Radiation Protection System vs. Conventional Apron and Shields in Clinical Interventional Procedures Open Journal of Radiology 03(03): 143-151.